STRUCTURAL RESEARCH SERIES NO. 8301

NSF/CEE-84035

PB85-149631

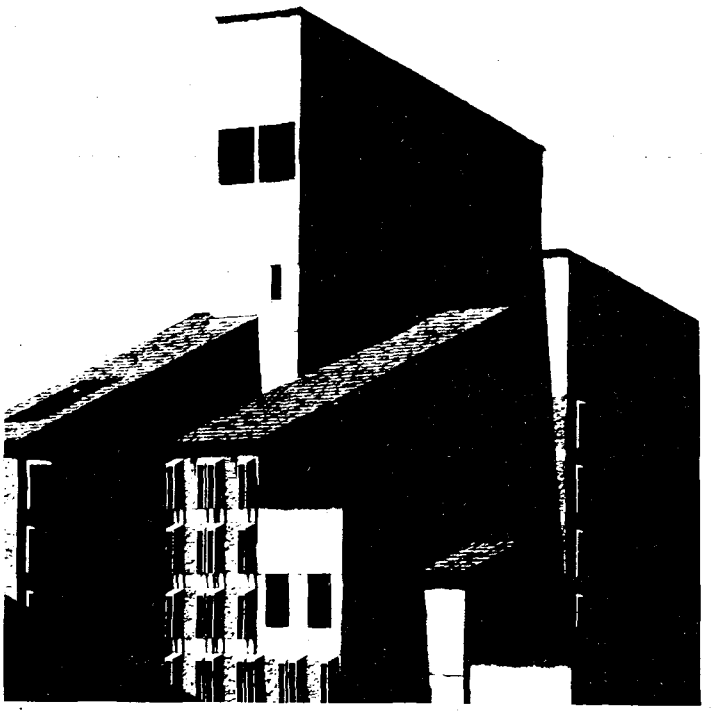

SCALE RELATIONSHIPS OF CONCRETE BEAM-COLUMN JOINTS

by Paul R. Phillco and Daniel P. Abrams

A Report to the National Science Foundation
Research Grants CEE-8119385 and PFR-8007094

Department of Civil, Environmental,
and Architectural Engineering

College of Engineering
and Applied Science

University of Colorado, Boulder

Structural Research Series No. 8301:

SCALE RELATIONSHIPS OF CONCRETE BEAM-COLUMN JOINTS

by

Paul R. Phillco

and

Daniel P. Abrams

A report to the

NATIONAL SCIENCE FOUNDATION

Research Grant CEE-8119385
and PFR-8007094

Department of Civil, Environmental, and
Architectural Engineering

College of Engineering and Applied Science

University of Colorado
Boulder

February 1984

ABSTRACT

The objective of this study was to investigate the ability of reduced-scale models of reinforced concrete beam-column joints to predict the response of large-scale prototypes. Six large-scale (approximately three quarter scale) specimens and six medium-scale (approximately one quarter scale) specimens were tested. Data from these tests were combined with data from tests of small-scale (approximately one-twelfth scale) specimens which were tested as part of a previous investigation. Each specimen was subjected to a reversed lateral load which was applied at the top of each column. Specimens of different scales were compared with regard to their load-rotation responses. Explicit scale factors based on the load-rotation relationship were derived.

ACKNOWLEDGEMENTS

The investigation described in this report was part of a continuing study of reinforced concrete structures subjected to earthquake motions. The work was funded by the National Science Foundation under grants PFR-8007094 and CEE-8119385. Experimental work was done at the Structural Research Laboratory at the University of Colorado.

The writers wish to express their appreciation to Professors Gerstle and Frangopol for their critical review of the manuscript, and to numerous graduate students, especially Bill Epp, Scott McNary, and Peter Waugh, for their support. Acknowledgement is also due to Dave Jones and his staff for assisting with the fabrication of the test apparatus.

This report was prepared as a thesis for the degree of Master of Science in Civil Engineering by Paul Phillleo under the direction of Daniel Abrams. Any opinions, findings, and conclusions or recommendations expressed in this publication are those of the authors and do not necessarily reflect the views of the National Science Foundation.

CONTENTS

CHAPTER

TABLES

Table

FIGURES

FIGURE

CHAPTER 1

INTRODUCTION

1.1 Objective and Scope

The overall objective of this experimental study was to examine the behavior of large-scale reinforced concrete beam-column joints and to compare the behavior with reduced-scale models. The test variables were the configuration and the size of the test specimens. Interior and exterior joints were tested and behavior of specimens at three different scales was studied.

Two large-scale exterior and four large-scale interior joints were constructed and subjected to lateral load reversals. An additional six interior joint specimens were constructed at medium- (1/4) scale and subjected to deflection histories similar to the large-scale specimens. One exterior and one interior joint were tested as a pilot test program by others (10). All other specimens were tested by this investigator. Small- (1/12) scale interior and exterior joints were tested at the University of Illinois (12). Steel and concrete properties and reinforcing ratios for all three scales were kept similar so direct comparisons between scales could be made.

This report pertains to all the testing of beam-column joint specimens at the University of Colorado. A description of test procedures are presented in Chapter 2. The responses of exterior

joint specimens and scale relationships of that component configuration are described in Chapter 3. A similar description for interior joints constitutes Chapter 4. Conclusions reached during the investigation, including recommendations for future scaling studies, are summarized in Chapter 5.

1.2 Related Research Elsewhere

Use of models to represent behavior of structures is not a new subject. The early Greeks and Romans used models to design structures in the absence of mathematical algorithms. In more recent times, models have been used to predict forces and deformations in beams, flat plates, box girders, and arch dams, to name only a few. In Europe, laboratories have been established for the specific purpose of model studies. Examples of these are the Laboratorio Nacional De Engenharia Civil in Portugal, the Instituto Sperimentale Modelli E Strutture in Italy, the Cement and Concrete Research Association in England, and the Institut fur Modellstatik at the University of Stuttgart.

In the United States and Japan, tests of small-scale building models have stimulated new research related to improved methods of analysis and design. A few examples of innovative improvements which have used test data from small-scale building models as a reference are noted in the following. Takeda (19) formulated complex behavior of reinforced concrete members subjected to load reversals with a set of rules so that nonlinear dynamic response could be calculated. Nonlinear analysis of reinforced concrete frames has been suggested as a design tool (22,23) using

similar hysteresis rules. Newmark (18) suggested a simplified analysis procedure using an elastic analysis with response spectra modified to include effects of inelastic response. Shibata and Sozen (20) proposed a design method that used a linear analysis to represent nonlinear behavior. A substitute structure with member stiffnesses chosen on the basis of nonlinear behavior was used with conventional modal analysis procedures. Biggs (21) has evaluated this approach with the inelastic response spectrum approach and the equivalent base shear approach. Further simplified analysis approaches include representing a MDOF structure with a SDOF model (24), and using modal analysis for bilinear systems (25). New trends to obtain a simple design criterion for reinforced concrete frame structures concentrate on simply limiting the drift (26) without an explicit description of the lateral forces.

Numerous building models have been subjected to simulated earthquake motions (2,3,4,5,7,8,9) at the University of Illinois. Other models have been tested in New Zealand (27) and California (28,29,15), and many tests will probably be done in the future. Small-scale components of some of these models have been tested by subjecting them to slowly applied loading reversals (12,13,14,30). Comparison of large-scale components (31,32,33,34,35,36,37, 38,39) with these small-scale components has been made but only qualitatively because specimen geometries, amounts of reinforcement, and loading patterns have not been kept consistent. The question of modeling was not an issue.

Past research on modeling of reinforced concrete behavior at a small scale is not new. A publication of the American Concrete Institute (40) summarizes work done in the sixties. Most of this work was not concerned with dynamic response, but rather direct scaling of materials to monotonically increasing loads. Work by Staffier (41) in the seventies addressed the problem of strain-rate effects on model reinforcement. Krawinkler (42) and Moncarz (43) investigated correlations between large and small-scale specimen response. Similar small-scale component models as those described at the University of Illinois (12,13,14,30) were tested. Their work did not study the sensitivities of response of a multistory structure to differences inherent in scaling at the component level. Verification of conclusions deduced from small-scale building tests was not within the scope of the research. Various model studies of multistory concrete buildings have been done in the People's Republic of China at the Academy of Building Research in Beijing (44).

Previously at the University of Colorado, Bedell and Abrams (11) studied scale relationships of concrete columns. A sustained axial force representing gravity loads was varied for different specimens to investigate differences in behavior attributable to inconsistent modeling of gravitational accelerations. Scale relationships were defined which showed the ratio of strengths of different scale specimens to be proportional to the square of the length scale factor for that particular component.

In a U.S.-Japan cooperative effort in Tsukba New Town, a full-scale seven-story building was tested to failure (1). As part of the effort, many subprojects have sprouted in the United States. These projects form a comprehensive study of testing reinforced concrete buildings for earthquake resistance. Large-scale components have been tested at the University of Texas. A one-fifth scale model was tested on an earthquake similator in California (47), while a one-tenth scale model was tested in Illinois (45).

Another multi-investigator research program was a study of the Imperial County Services Building in El Centro, California which was damaged severely by an earthquake in 1979. Large-scale components of this building have been tested in California. A one-tenth scale model was tested on an earthquake similator in Illinois to test the usefulness of small-scale models in estimating response of full-scale structures (46).

CHAPTER 2

OUTLINE OF EXPERIMENTAL WORK

2.1 Introductory Remarks

Two exterior and four interior large-scale beam-column joint specimens, and six interior medium-scale specimens were tested as outlined in the first chapter. This second chapter presents details of specimen design, fabrication, instrumentation, and test procedures used for the tests. In addition, figures showing the dimensions and details of the small-scale specimens tested at the University of Illinois are included so the reader may compare specimens at different scales. A summary of all specimens tested is given in Table 2.1.

2.2 General Configuration of the Test Specimens

The configuration of each beam-column joint was chosen so that forces would be transferred across the specimen similarly to those transferred in a similar element in a multi-story frame structure. Boundary conditions at the ends of the beams and columns were chosen to replicate idealized points of contraflexure in a laterally loaded frame. A horizontal load P was applied at the top of the column (Fig. 2.1) which represented the story shear. A pin connection at the base of the column, and a roller support at the end of each beam simulated appropriate restraint conditions.

TABLE 2.1

SUMMARY OF SPECIMENS TESTED

SPECIMEN TYPE	SCALE	INVESTIGATOR	NUMBER TESTED
Exterior Joint	Large	Stewart (1)	1
Interior Joint	Large	Stewart	1
Exterior Joint	Small	Kreger (2)	5
Interior Joint	Small	Kreger	4
Exterior Joint	Large	Philleo	1
Interior Joint	Large	Philleo	3
Interior Joint	Medium	Philleo	6

(1) Stewart, J. and Abrams, D.P., "Comparison of Large and Small-Scale Reinforced Concrete Behavior", Masters Thesis, University of Colorado, July, 1982.

(2) Kreger, M.E. and Abrams, D.P., "Measured Hysteresis Relationships for Small-Scale Beam-Column Joints", Civil Engineering Studies, Structural Research Series No. 453, University of Illinois, Urbana, August, 1978.

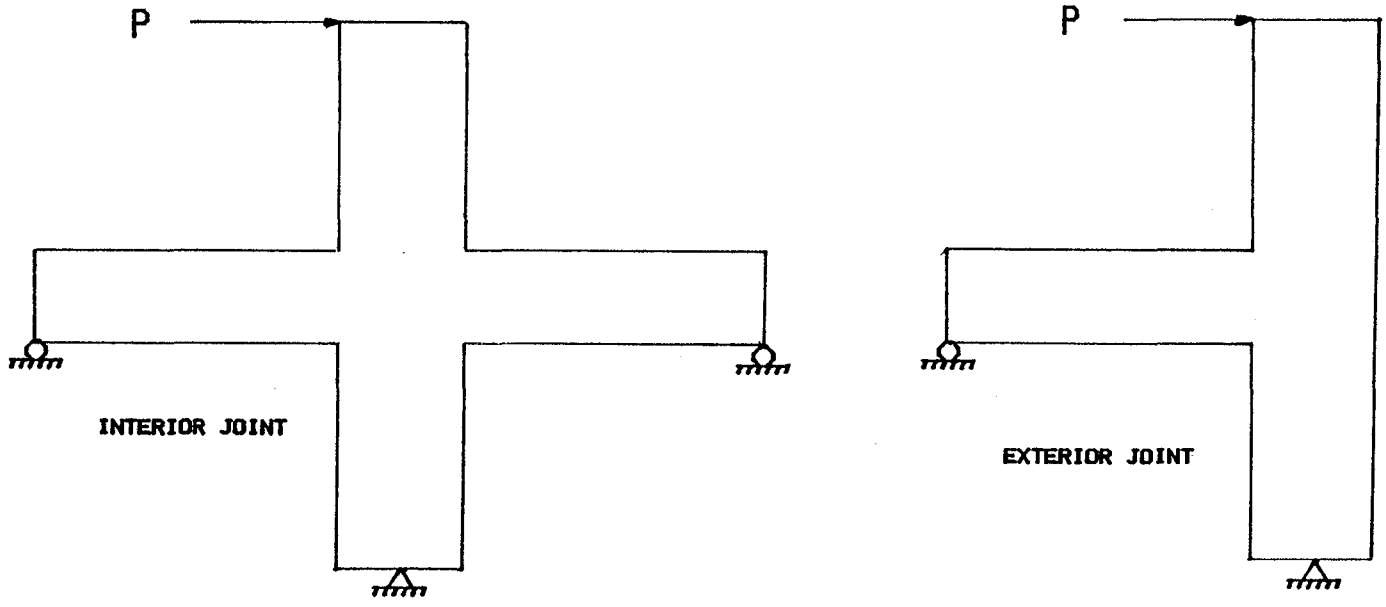

Fig. 2.1 Configuration of Test Specimens

Column and beam lengths were chosen to replicate ratios of moment-to-shear in an actual frame, and equaled one-half of story heights or bay widths. Proportioning of flexural strengths was done so that the beams would be weaker than the columns. Nonlinear behavior was expected to occur at the ends of the beams while the column was expected to crack but not yield.

2.3 Description of the Large-Scale Specimens

Specimens dimensions are shown in Fig. 2.2. The large-scale specimens were nine times larger than the small-scale specimens, which was equivalent to 3/4 scale; however, large-scale specimens were considered to be full size because reinforcing bars were #5 or #6, cross sections were at least 343 x 343 mm (13.5 x 13.5 inches), and the maximum aggregate size was 20 mm (3/4 inch). To define the exact scale any closer would require a firm definition of a standard beam or column size which would be meaningless.

Amounts of longitudinal reinforcement in the beams and columns of five large-scale specimens (Fig. 2.3) were chosen to match reinforcing ratios in the small-scale specimens (Fig. 2.3). Beams were reinforced with three #6 bars on the top and bottom faces (area of steel on one face was equal to .84% of the effective depth times the width). Columns were reinforced with eight #5 bars (area of steel was equal to 1.02% of the gross cross sectional area). The beams in the sixth specimen were reinforced with five #4 bars on each face (Fig. 2.3). This area of steel was slightly less (.62%) than the others, but corresponded to the maximum number of bars allowed by ACI provisions (16). The reinforcement was changed

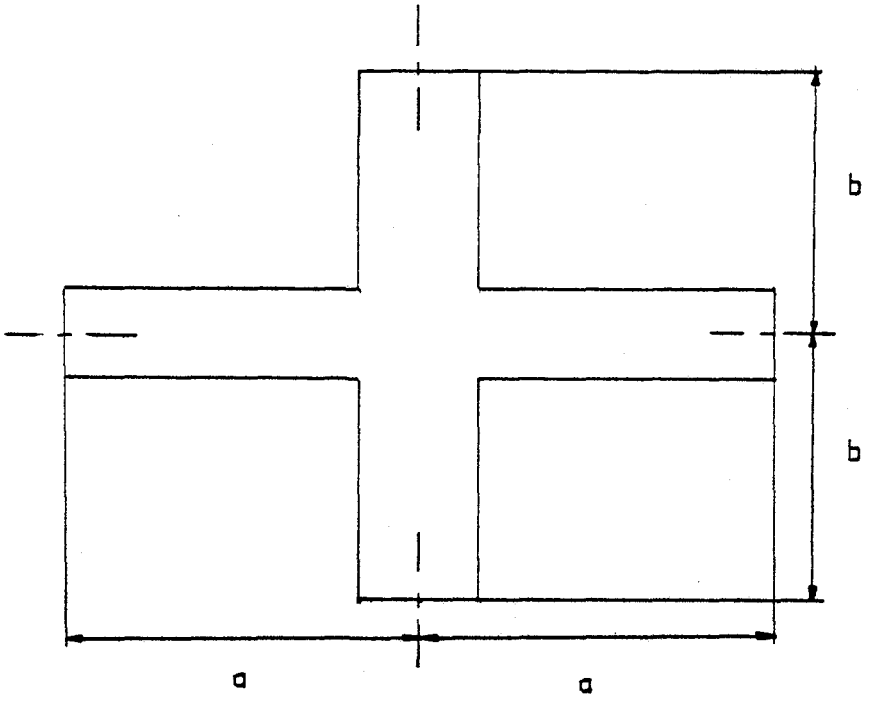

	a	b
Large Scale	1370 mm	1030 mm
Medium Scale	457 mm	343 mm
Small Scale	152 mm	114 mm

Fig. 2.2 Specimen Dimensions

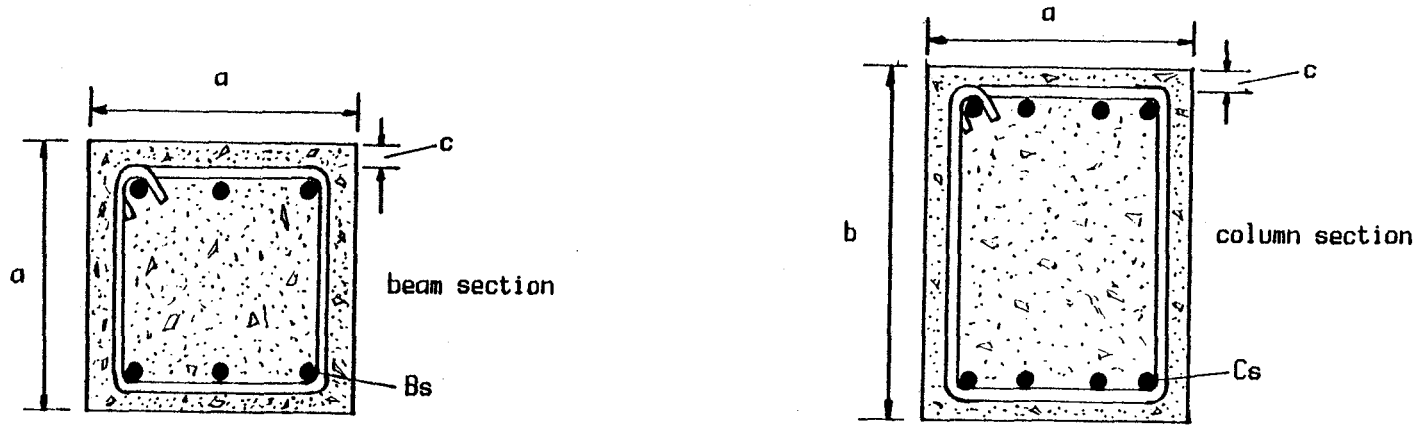

	a	b	c	Bs	ρ_{beam}	Cs	$\rho_{col.}$
Large-Scale	343 mm	457 mm	38 mm	3 #6 bars	.84 %	4 #5 bars	1.02 %
Large-Scale, LIJ4	343 mm	457 mm	38 mm	5 #4 bars	.62 %	4 #5 bars	1.02 %
Medium-Scale	114 mm	152 mm	13 mm	2 #3 bars	1.00 %	3 #3 bars	2.40 %
Small-Scale	38 mm	51 mm	5 mm	2 #13g wire	.71 %	3 #13g wire	1.33 %

Fig. 2.3 Beam and Column Cross Sections

in this specimen to investigate the effect of bar development length on the steel-concrete bond within the joint region. The column reinforcement in the sixth specimen was identical to the other five.

Symmetrical layers of beam reinforcement were not representative of an actual structure which would be governed by gravity loadings, but was done so that behavior could be compared with the small-scale specimens. Column shears for the interior joint specimen were expected to be twice those for the exterior joint specimen, however the same reinforcement was used for each because axial forces in an actual structure subjected to lateral loads would be much larger in the exterior than interior columns. Although the effect of column axial load was not part of this investigation, proper replication was felt necessary for correlations with possible future studies.

Stirrups and ties were provided with a high factor of safety similar to that used in the design of the small-scale specimens. In all six large-scale specimens, #3 closed hoops were used in the columns and beams (Fig. 2.4), and were spaced according to ACI requirements (16).

Forces were transferred to the specimens by means of steel "T" sections which were bolted to embedded plates (Fig. 2.5 and 2.6). The plates were tied to the longitudinal reinforcing bars in the beam or column, and were held in place during casting by bolts. These bolts were removed when the forms were stripped. This detail enabled the "T" sections to be used on all six specimens. Roller bearings were press-fitted to a hole in the "T" sections to produce

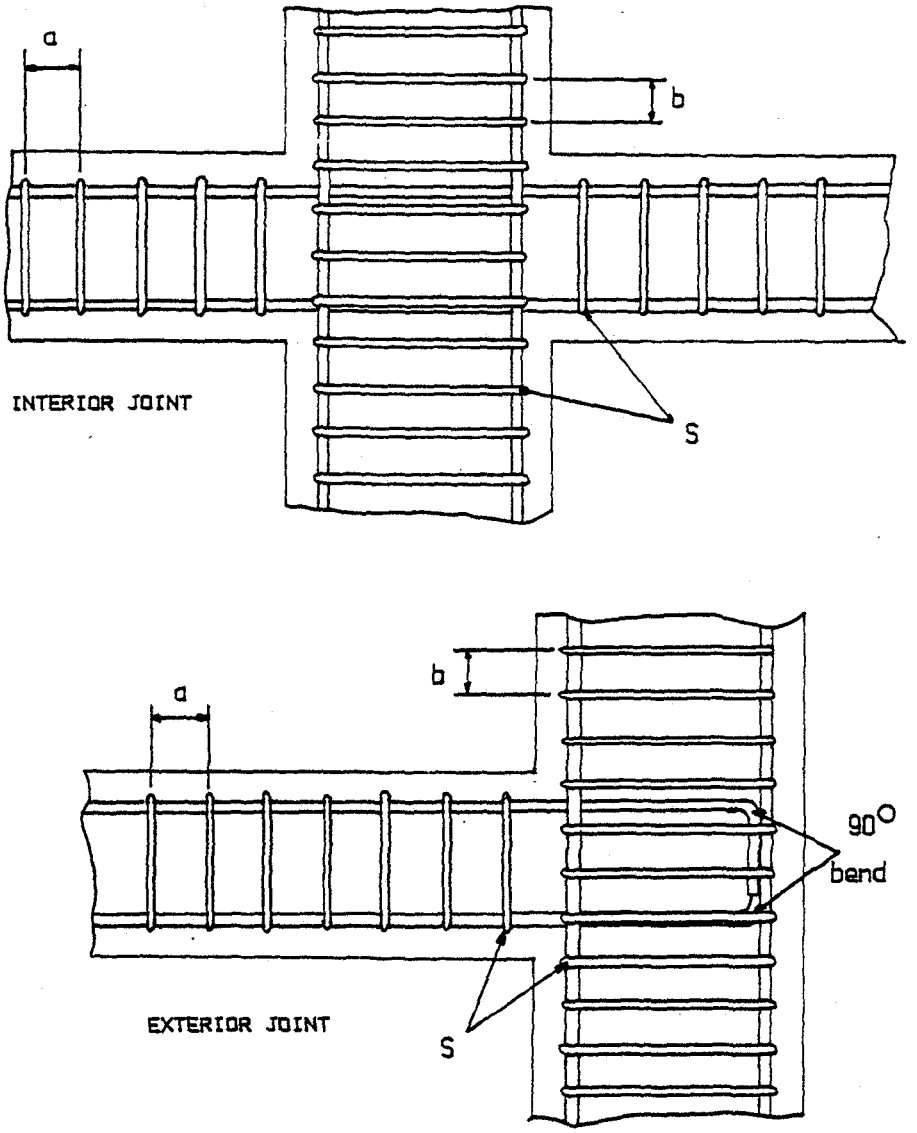

	a	b	S
Large-Scale	102 mm	76 mm	#3 closed hoops
Medium-Scale	34 mm	25 mm	#9g wire closed hoops
Small-Scale	11 mm	8 mm	#16g wire spirals

Fig. 2.4 Shear Reinforcing Detail

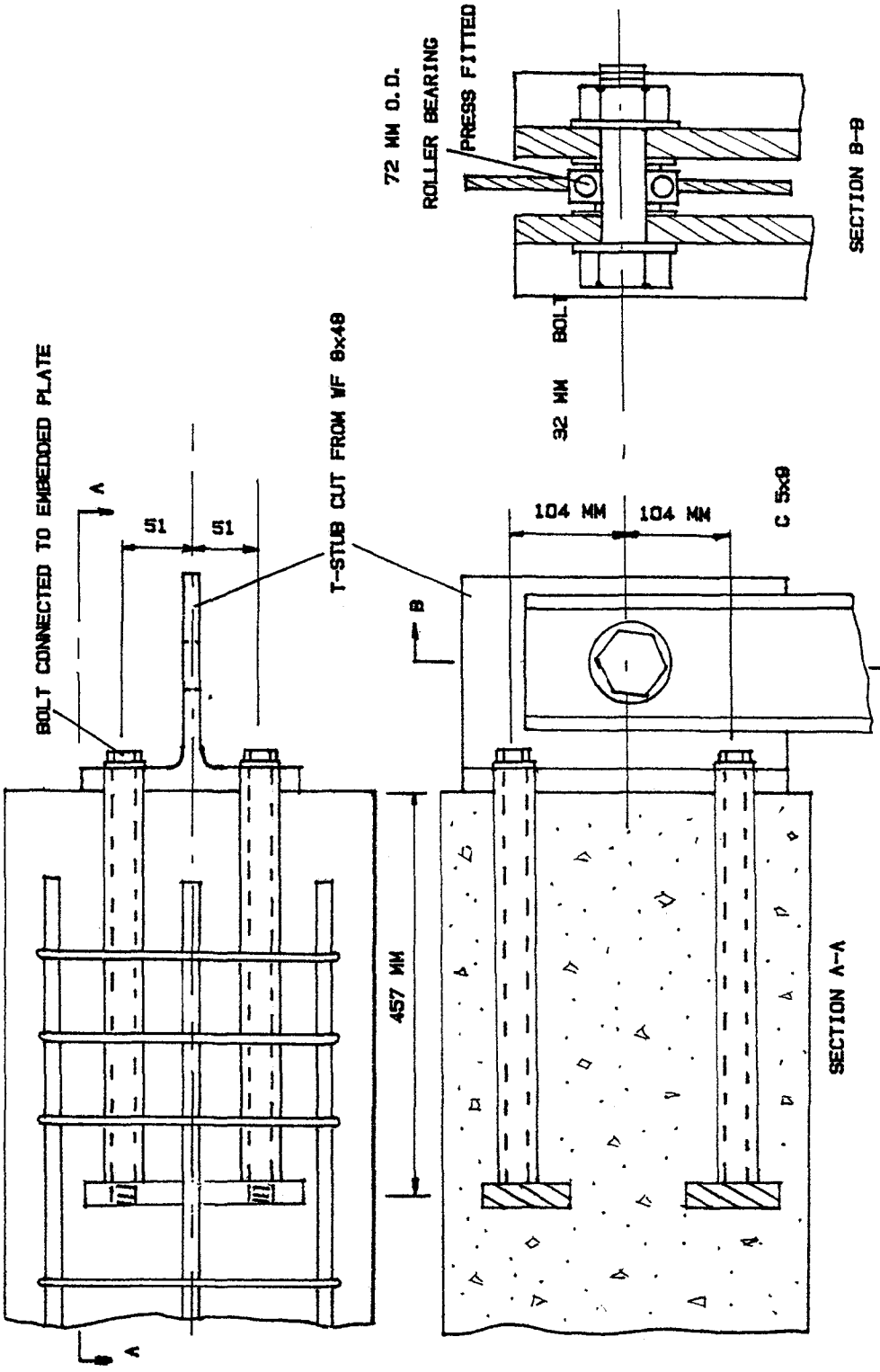

Fig. 2.5 End Connections for Large-Scale Specimens

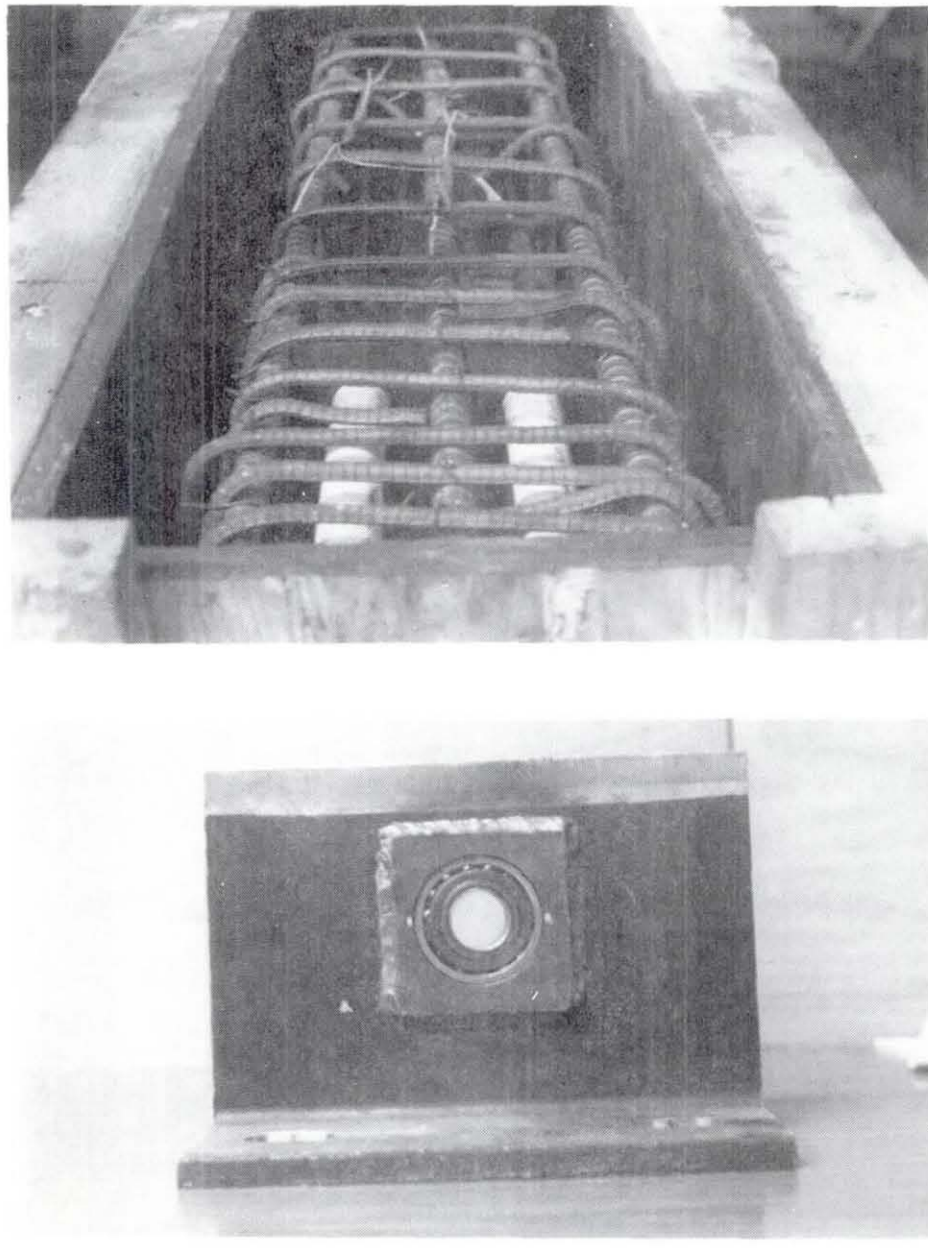

Fig. 2.6 Details of End Connections

the pin connection at the column base and beam ends (Fig. 2.6).

2.4 Description of the Medium-Scale Specimens

The medium-scale specimens were three times larger than the small-scale specimens, which was equivalent to 1/4 scale (Fig. 2.2). These specimens were designed to be the smallest possible into which conventional reinforcing bars would fit for longitudinal reinforcement. The beams (Fig. 2.3) were reinforced with two #3 bars on the top and bottom faces (area of steel equaled 1% of concrete area). The columns were reinforced with six #3 bars (area of steel equaled 2.4% of concrete area). The columns were heavily reinforced to make sure they remained much stiffer than the beams. Shear reinforcement was provided by #9 gage wire which was cut from a spool and bent to form closed hoops (Fig. 2.4). Stirrup and tie spacing was scaled down from the large-scale design and therefore coincided with the ACI seismic design provisions (16).

Forces were transferred to the medium-scale specimens by means of holes through the specimen which were lined with steel conduit. A bolt extended through these holes and through ball bearings that had been press-fitted into supporting channels. When properly connected, the specimen could rotate about the ball bearing, thus producing the necessary pin connections at the beam and column ends. The medium-scale test apparatus will be discussed in more detail in Section 2.7.

2.5 Materials

The concrete used in the large-scale specimens was manufactured and delivered by a local pre-mix concrete firm. Type 1 Portland Cement was used and the maximum aggregate size was 20 mm (3/4 inch). The mix proportions by weight were .6:1:2.8:3.6 (water: cement: fine aggregate: coarse aggregate). The concrete used in the medium-scale specimens was designed and manufactured in the laboratory. Again Type 1 Portland Cement was used, but the maximum aggregate size was scaled down to 7 mm (1/4 inch). The mix proportions by weight were .5:1:2:2.2. Physical properties of the concrete were determined from samples taken during casting and tested one day after each specimen was tested. The measured stress-strain characteristics of the concrete are presented in Fig. 2.7a. Compressive tests were done on 152 by 205 mm (6 by 12 inch) cylinders in a 1300 kN (300 kip) testing machine. Compressive strains in the concrete were measured with a mechanical dial gage sensitive to .03 mm (.001 inch) over a gage length of 127 mm (5 inches). Modulus of rupture tests were done in a 45 kN (10 kip) testing machine, and split cylinder tests were done in the 1300 kN testing machine.

The reinforcing bars, hoops, and wire were purchased from a local manufacturer. The longitudinal reinforcing steel consisted of deformed bars conforming to ASTM A-615 Specification for Grade 60 steel. The stress-strain characteristics are presented in Fig. 2.7b. These tests were done in a 500 kN (100 kip) capacity load frame operated in strain control at a rate of .0005 per second.

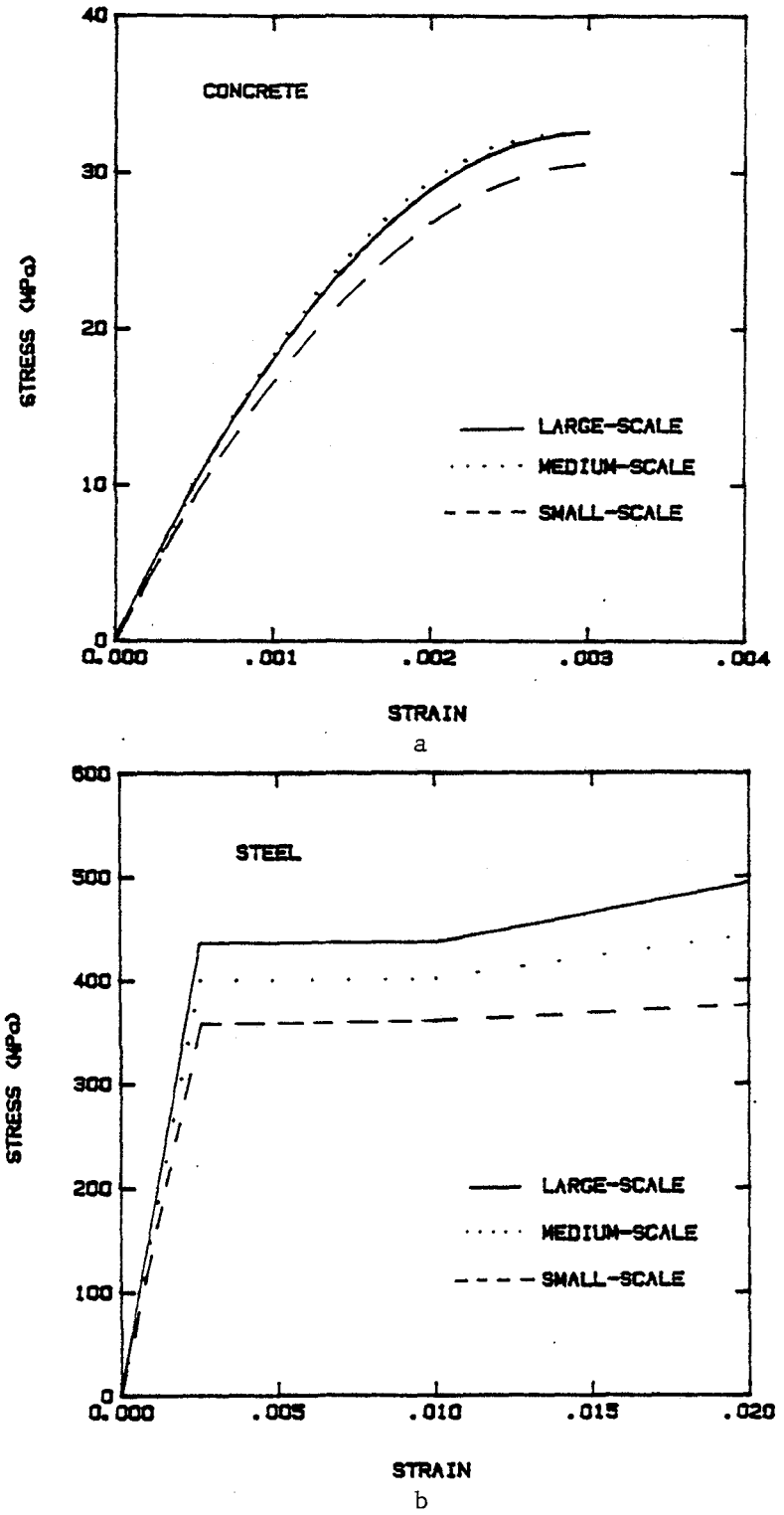

Fig. 2.7 Measured Properties for (a) Concrete and (b) Steel

Strain was related to elongation of the bar measured over a 25 mm (1 inch) length.

2.6 Fabrication

The reinforcing cages were secured together with #16 gage wire ties. Conventional reinforcing chairs were used to hold the cage in position during casting. The large-scale specimens were cast upright in plywood forms stiffened with battens (Fig. 2.8). The medium-scale specimens were cast flat in wood forms with one side exposed (Fig. 2.8). The concrete was compacted with a high frequency vibrator. Cylinder and prism samples were taken intermittently during casting. All specimens and samples were cured under moistened burlap for seven days, at which time the forms were removed. Thereafter the specimens were air cured until the testing date, 28 days after casting.

2.7 Test Apparatus

Each specimen was loaded with an apparatus which was designed to simulate the transfer of forces through actual building elements. Diagrams of the apparatus used to test large, medium and small-scale specimens are presented in Figs. 2.9-2.11. For the large and medium-scale tests, load was applied with a 156 kN (35 kip) ram which was mounted on a concrete reaction-block structure. The reaction block was constructed of four modules which were prestressed to the test floor. The ram was controlled electronically so that lateral displacement of the top of the column would be at a constant rate. This provided a safeguard against

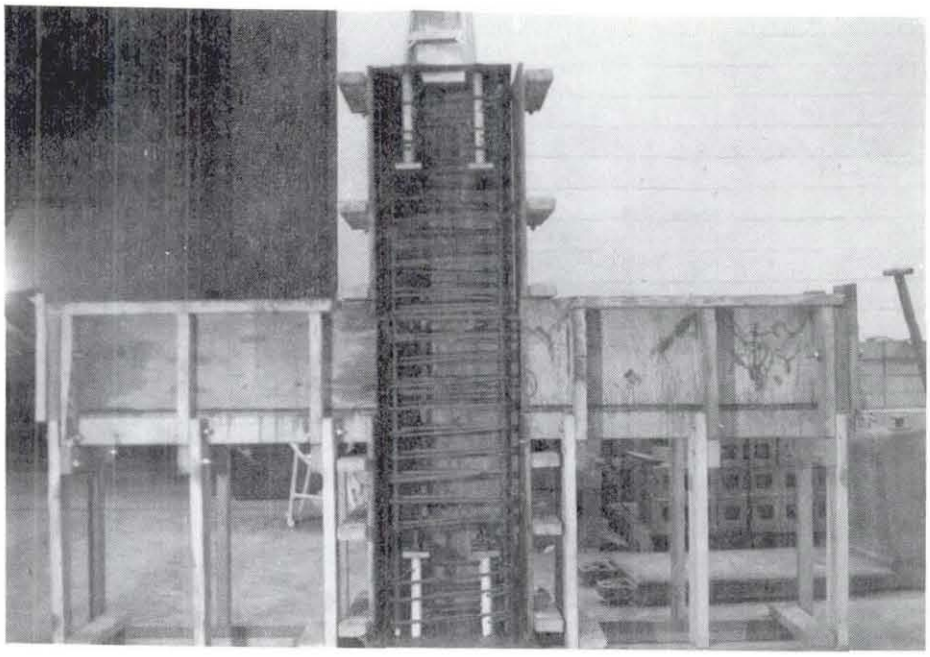

a

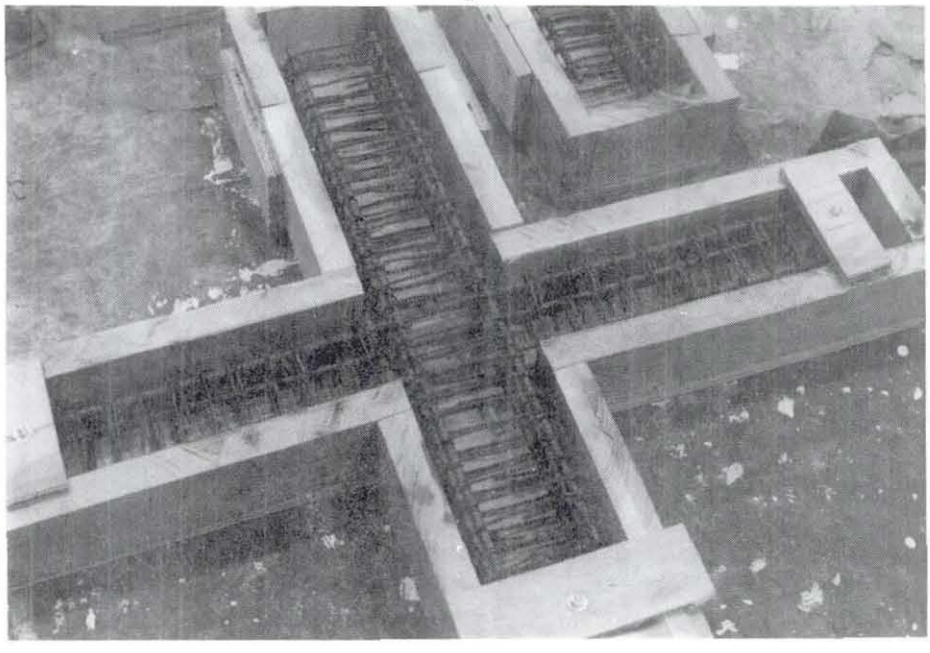

b

Fig. 2.8 Formwork for (a) Large and (b) Medium-Scale Specimens

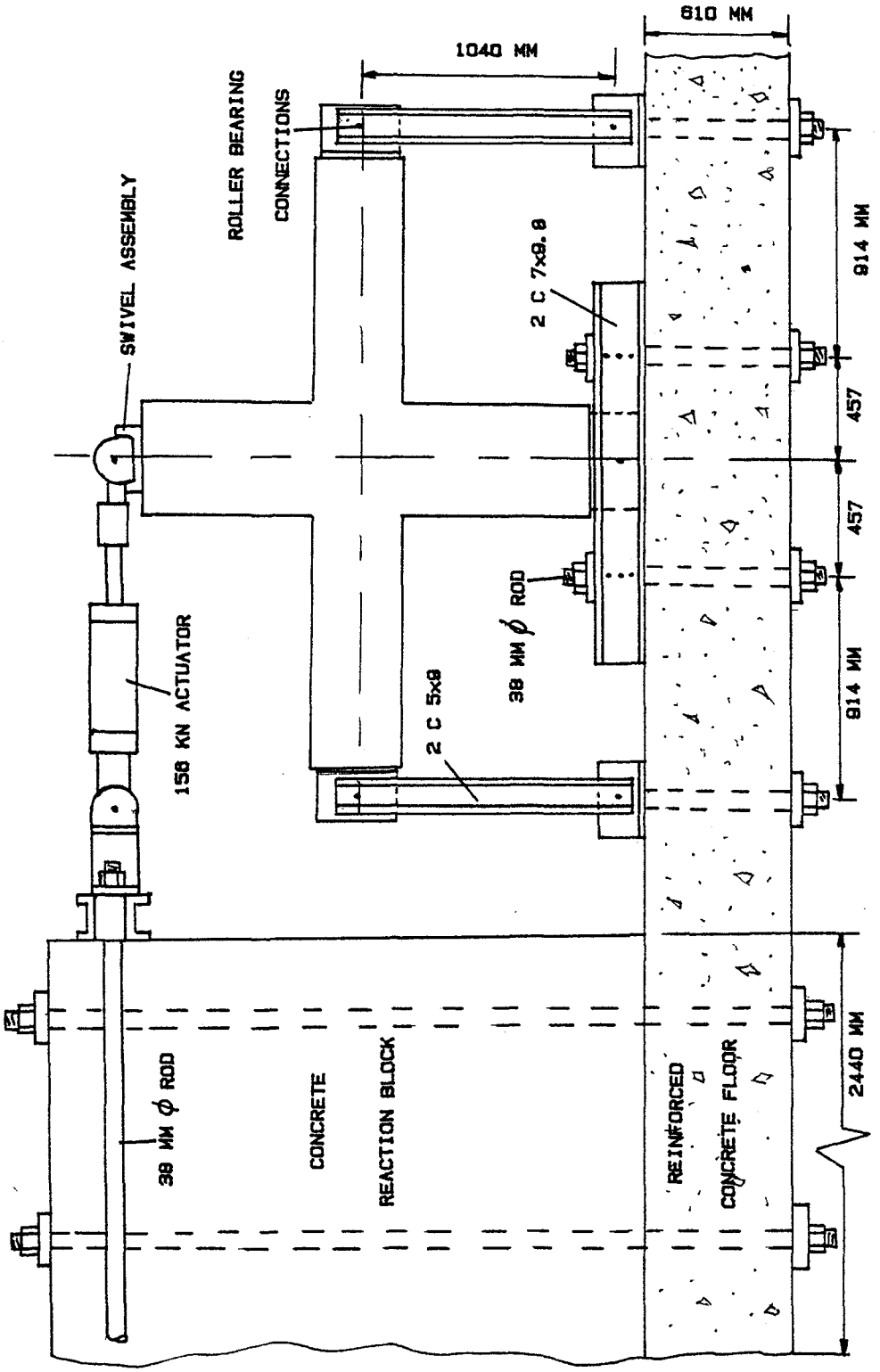

Fig. 2.9 Large-Scale Test Apparatus

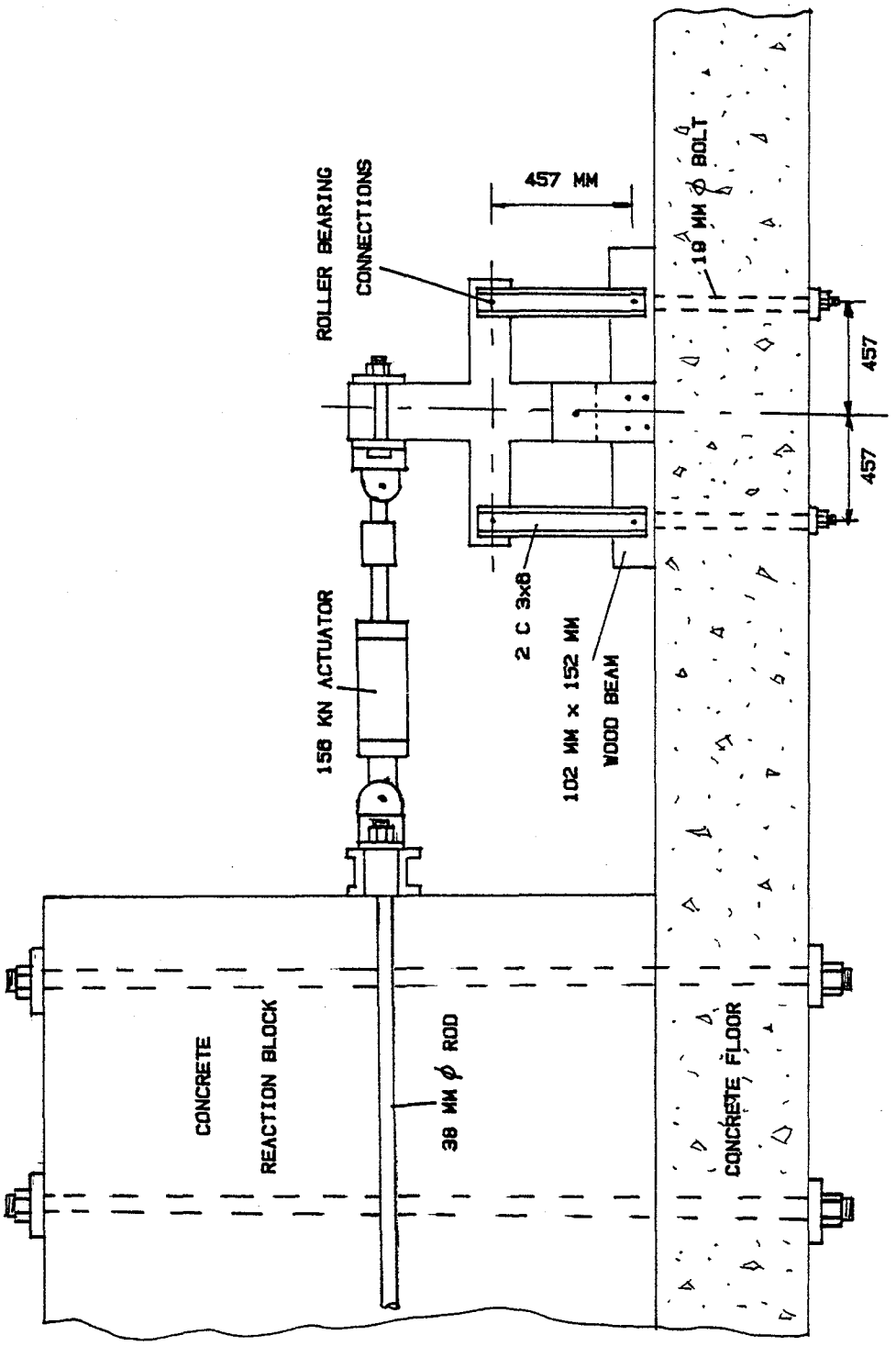

Fig. 2.10 Medium-Scale Test Apparatus

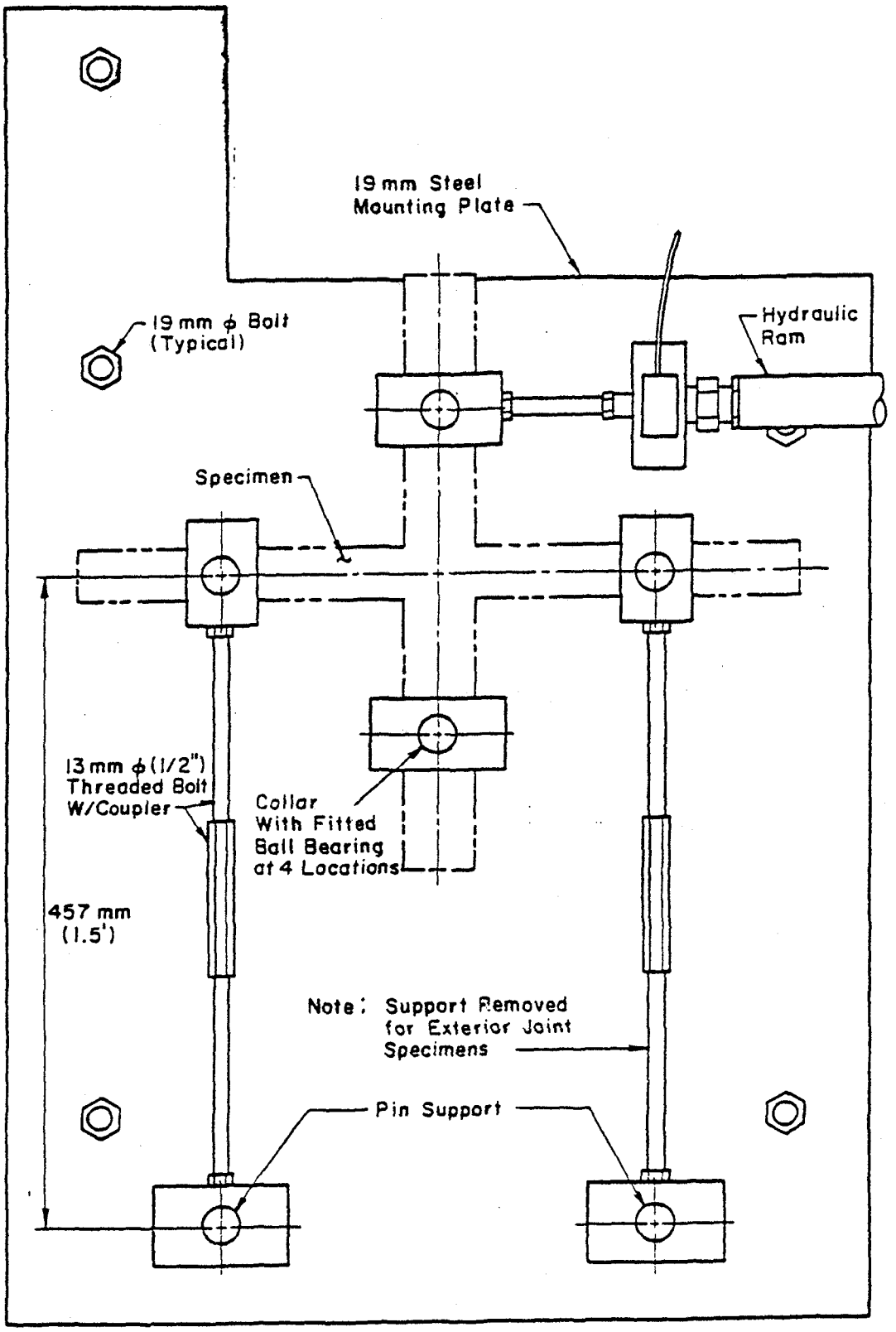

Fig. 2.11 Small-Scale Test Apparatus, from Kreeger (12)

excessive instantaneous damage if a specimen were to suddenly loose strength.

The ram was connected to the specimen with a swivel head which permitted rotation in the vertical and horizontal planes with negligible resistance. Swivel heads were located on each end of the ram so that transverse forces would not exist across the ram and possibly load the specimen out of plane. Roller supports were simulated at the ends of the beams using a set of steel channels which were connected at the top and bottom to fixtures with roller bearings. For the range of lateral displacement used in this test series, the channels permitted horizontal movement with negligible resistance and essentially no vertical movement. Out of plane movements of the specimens were prevented with a set of cables and turnbuckles which were attached to the beam ends and secured to the test floor at an angle of 33 degrees with the horizontal.

2.8 Instrumentation

For all specimens, applied load, joint rotation, load-level displacement, and rotation at beam ends were measured (Fig. 2.12). In addition, the strains in the reinforcement in the large-scale specimens were measured. The applied load was measured with the 156 kN (35 kip) capacity load cell with a sensitivity of 0.1%. The joint rotation was measured using a pair of 127 mm (5 inch) LVDT's. A rigid aluminum bar, 1830 mm (72 inches) for the large-scale, and 686 mm (27 inches) for the medium-scale was secured to the joint region on each side of the specimen. A rigid rod connected these aluminum bars to the core of the LVDT. The load-level displacement

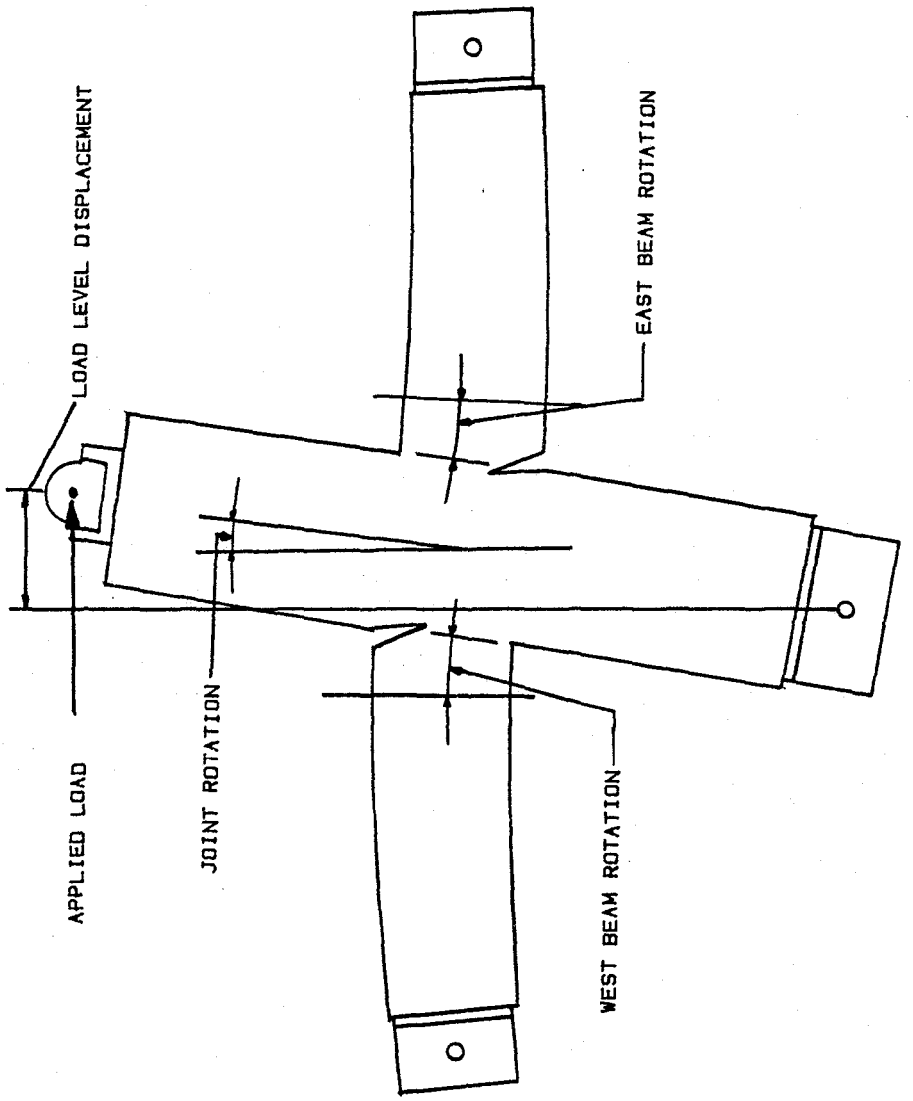

Fig. 2.12 Description of Physical Quantities Measured

was measured with a 102 mm (4 inch) LVDT in a similar arrangement (Fig. 2.13).

Inelastic rotations within a specified gage length of 152 mm (6 inches) for the large scale, and 76 mm (3 inches) for the medium scale, at the ends of the beams were measured. One 25 mm (1 inch) LVDT was mounted on the top and bottom faces of each beam and attached to the column face. Swivel connections were provided so that free rotation of the LVDT and the core was possible (Fig. 2.14). All displacement transducers had sensitivities of less than .5 of the range of the particular instrument. Prior to testing, each transducer was calibrated on a vertical milling machine sensitive to .003 mm (.0001 inch).

Strains in the longitudinal reinforcement in the large-scale specimens were measured at locations indicated in Fig. 2.15. Strain gages were attached to the middle reinforcing bar in each beam.

Voltage outputs from the load cell, LVDT's, and strain gages were fed into an analog-digital converter. The resulting binary coded number was read by a Hewlett-Packard 9825T computer which then stored the number permanently on magnetic tape. Following testing, the numbers on tape were converted to measurements by the 9825T, and plotted using a Hewlett-Packard 7225B plotter.

2.9 Testing Procedure

Each large and medium-scale specimen was loaded through repeated cycles of ever increasing rotation (Fig. 2.16). The first six cycles led up to the yield load, and the remaining cycles represented loading in the post-yield region. Joint rotation was

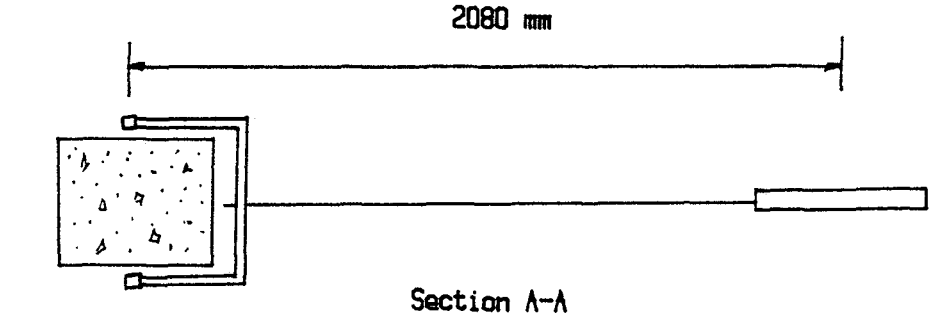

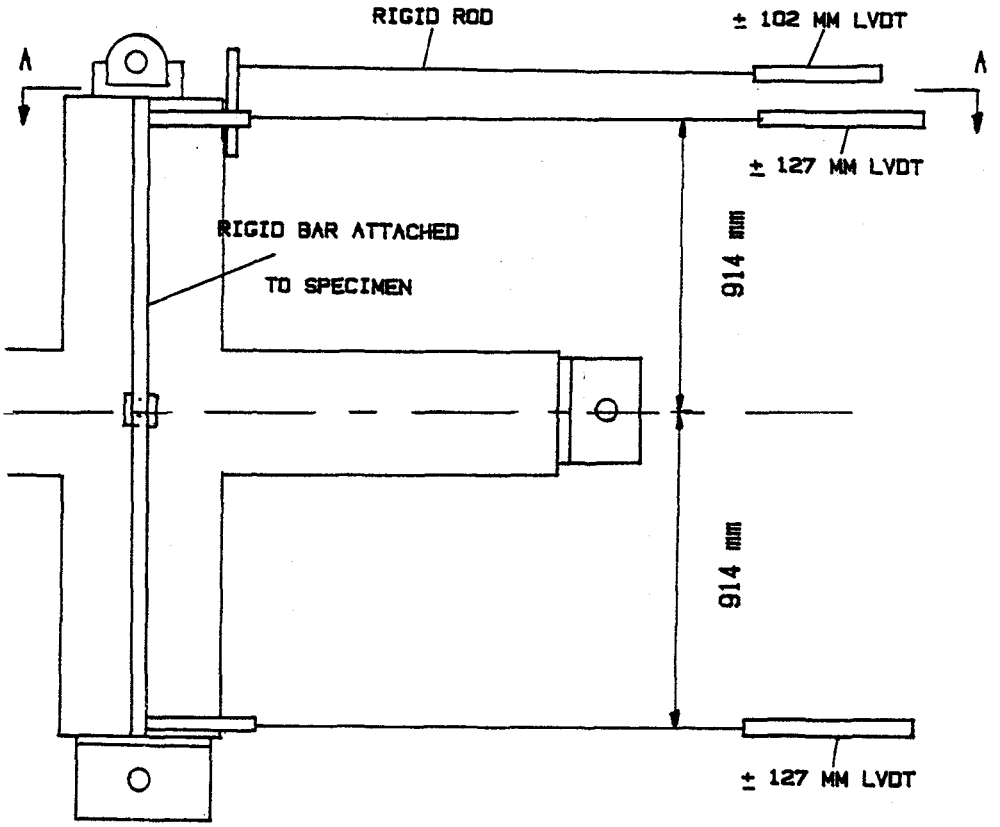

Fig. 2.13 Instrumentation

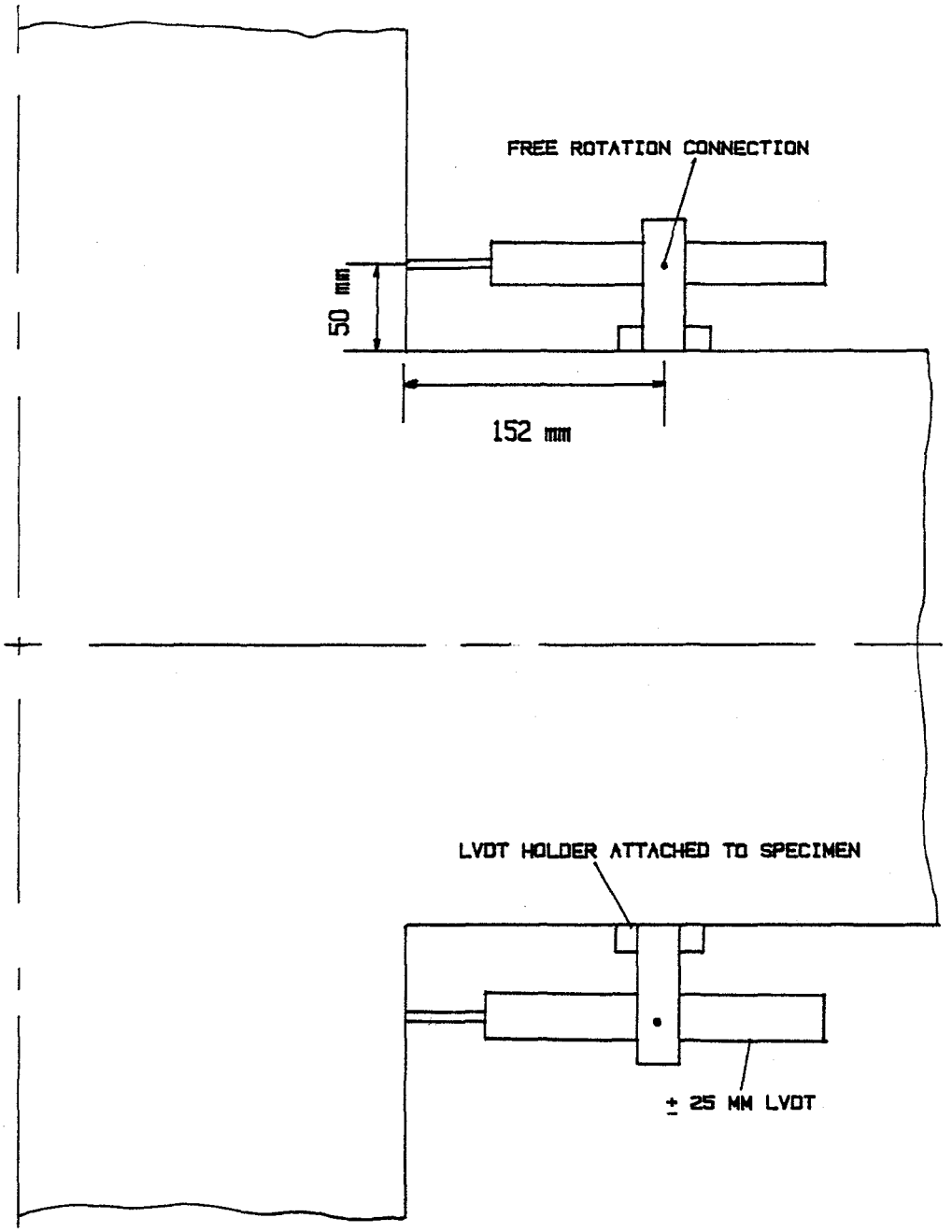

Fig. 2.14 Beam Rotation LVDT Arrangement

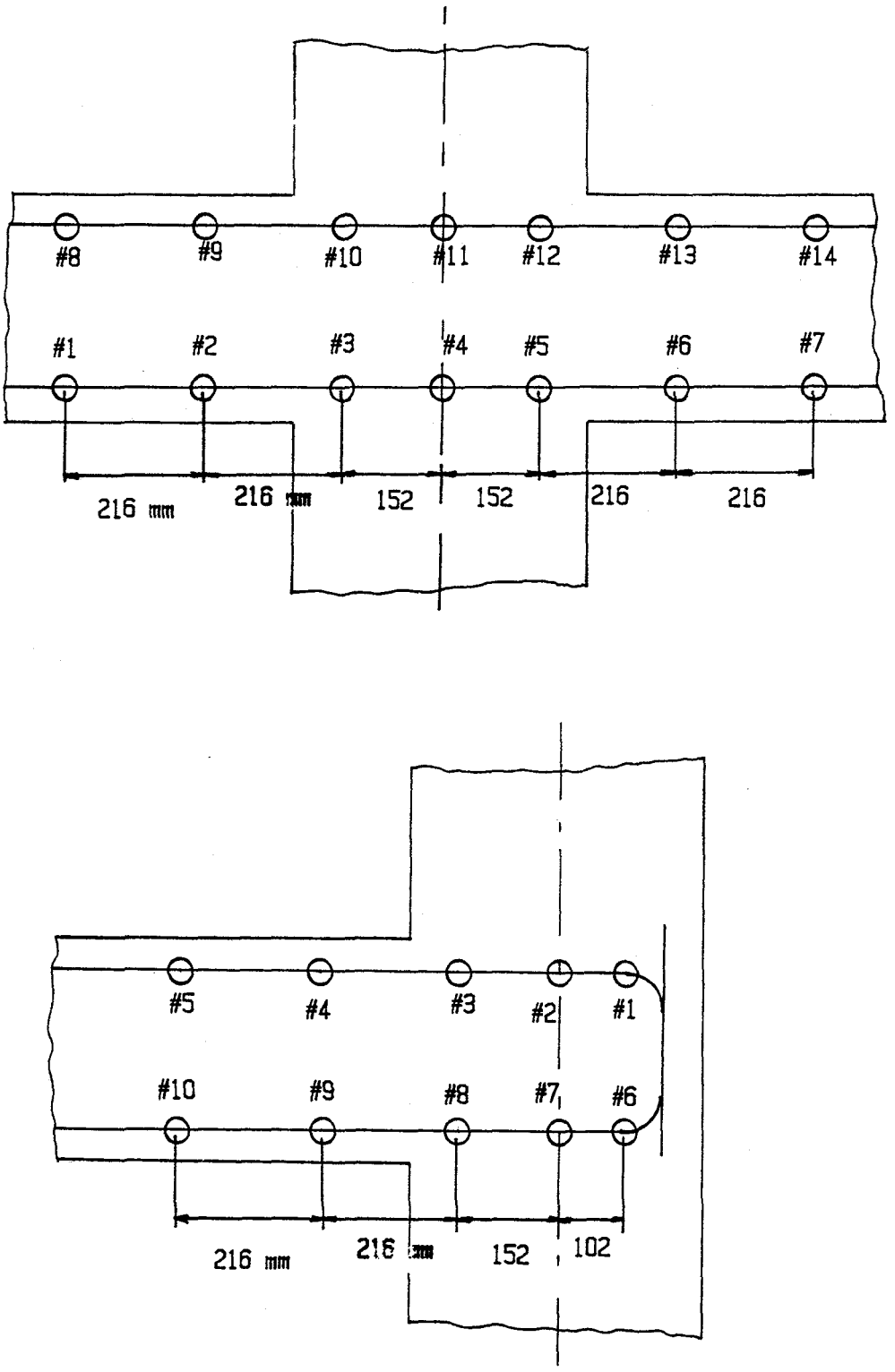

Fig. 2.15 Location of Strain Gages in Large-Scale Specimens

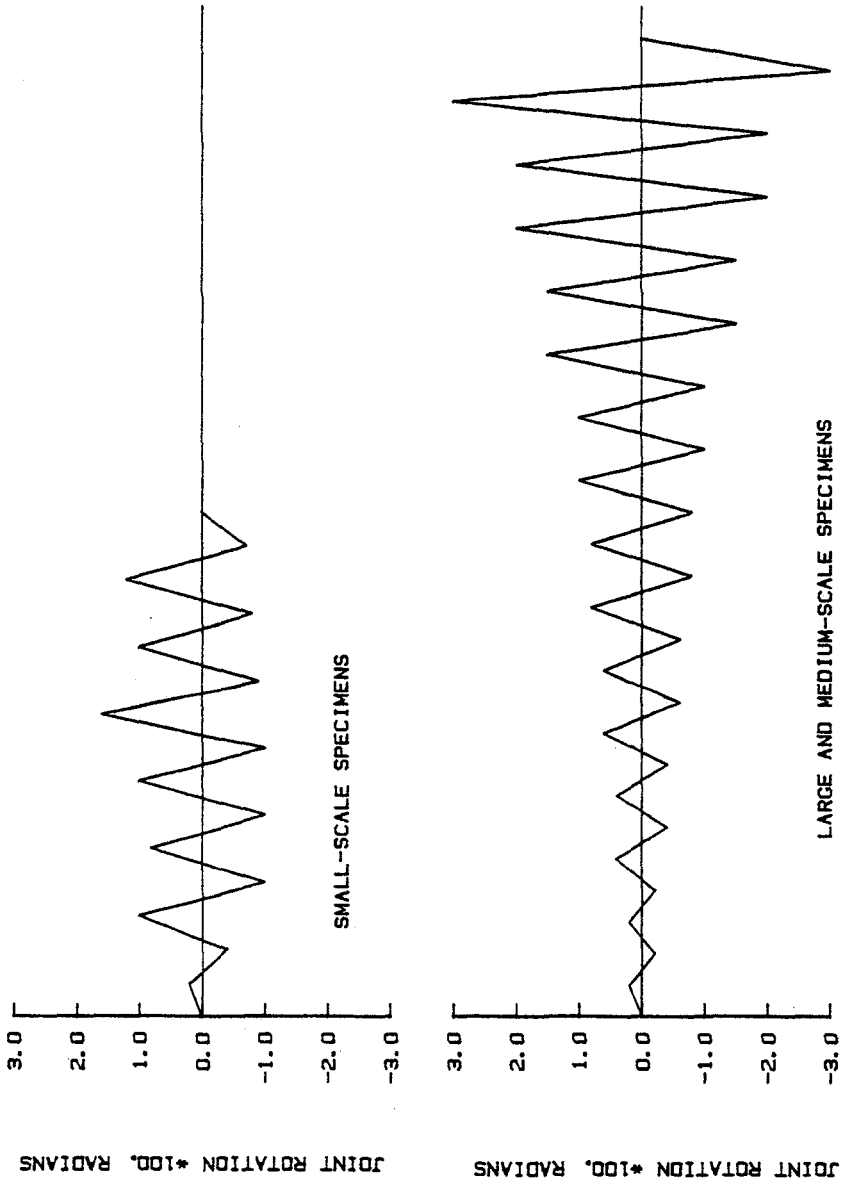

Fig. 2.16 Displacement Histories

the controlling variable due to its non-dimensional nature.

The tests were monitored by a continuous plotting of load versus rotation and load versus load-level displacement. All measured parameters were read at intervals such that a smooth curve could be obtained later when the data were reduced. Crack patterns were photographed at the end of each cycle, and at maximum rotations for large-amplitude cycles. Widths of significant cracks were recorded at maximum positive, negative, and zero rotations. Each test took approximately eight hours to complete.

CHAPTER 3

SCALE RELATIONSHIPS OF EXTERIOR JOINTS

3.1 Introduction

This chapter is a description of how accurately the response of a large-scale exterior joint was predicted by its small-scale counterpart. Because the large-scale specimen so nearly resembled an actual building element, it was considered the control in this investigation. Its response is described in detail here, then the response of the small-scale specimen is compared to it. The reader should recall no medium-scale exterior joints were tested. This was because the mechanisms exhibited by the exterior joints were simple compared to those in the interior joints, so it was felt further investigation of the exterior joint at medium scale was not necessary.

3.2 Description of Large-Scale Specimen Response

The load-rotation curve for a large-scale specimen is shown in Fig. 3.1. It is divided into two graphs for a clearer presentation. Curves showing load-displacement, load-rotation at the beam end, and load-strain relationships are shown in Figs. 3.2-3.3. Photographs of damage in the joint region are shown in Fig. 3.4. Measured widths of significant cracks are listed in Fig. 3.5. The data from just one specimen is presented because the

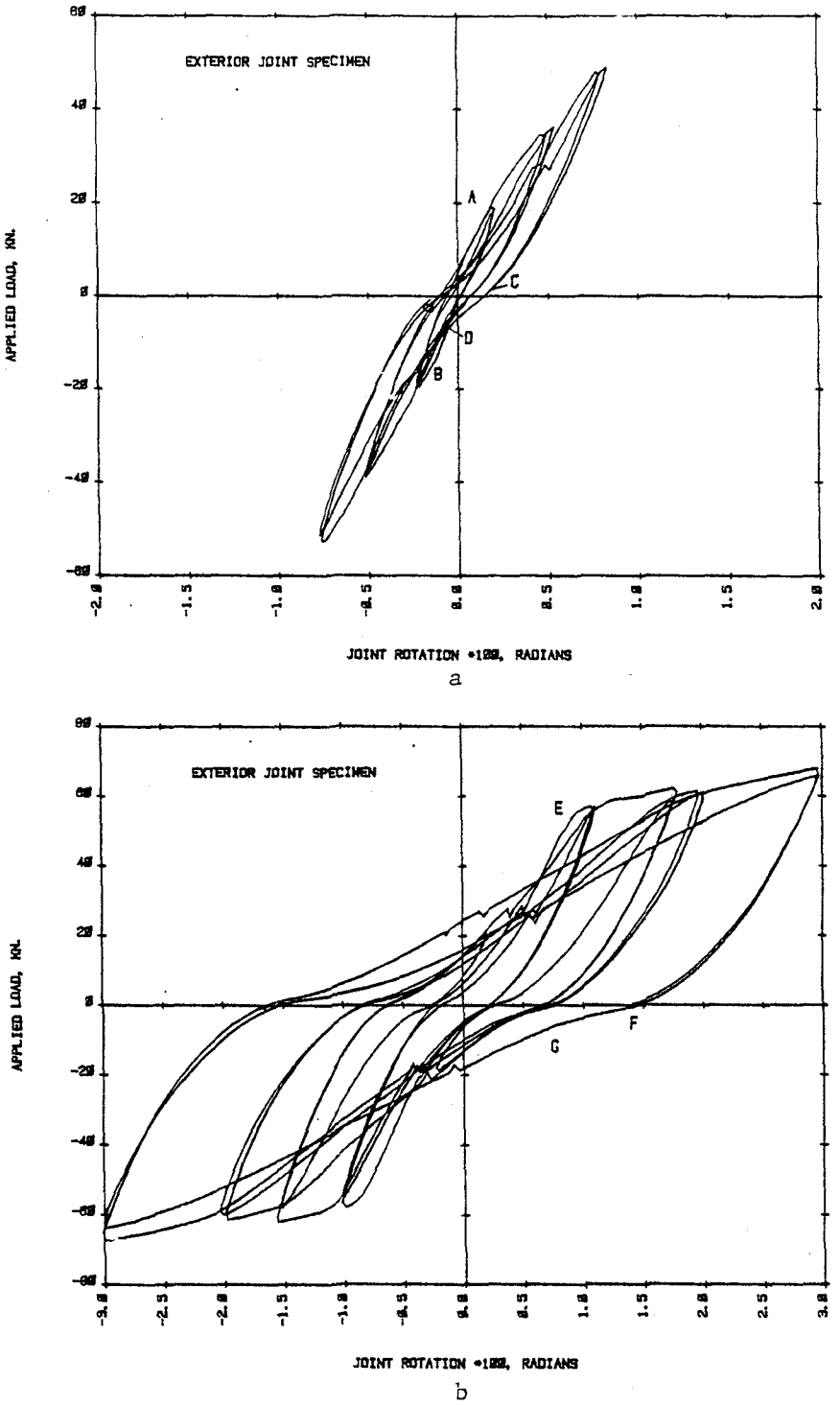

Fig. 3.1 Load-Rotation Response for Exterior Joint

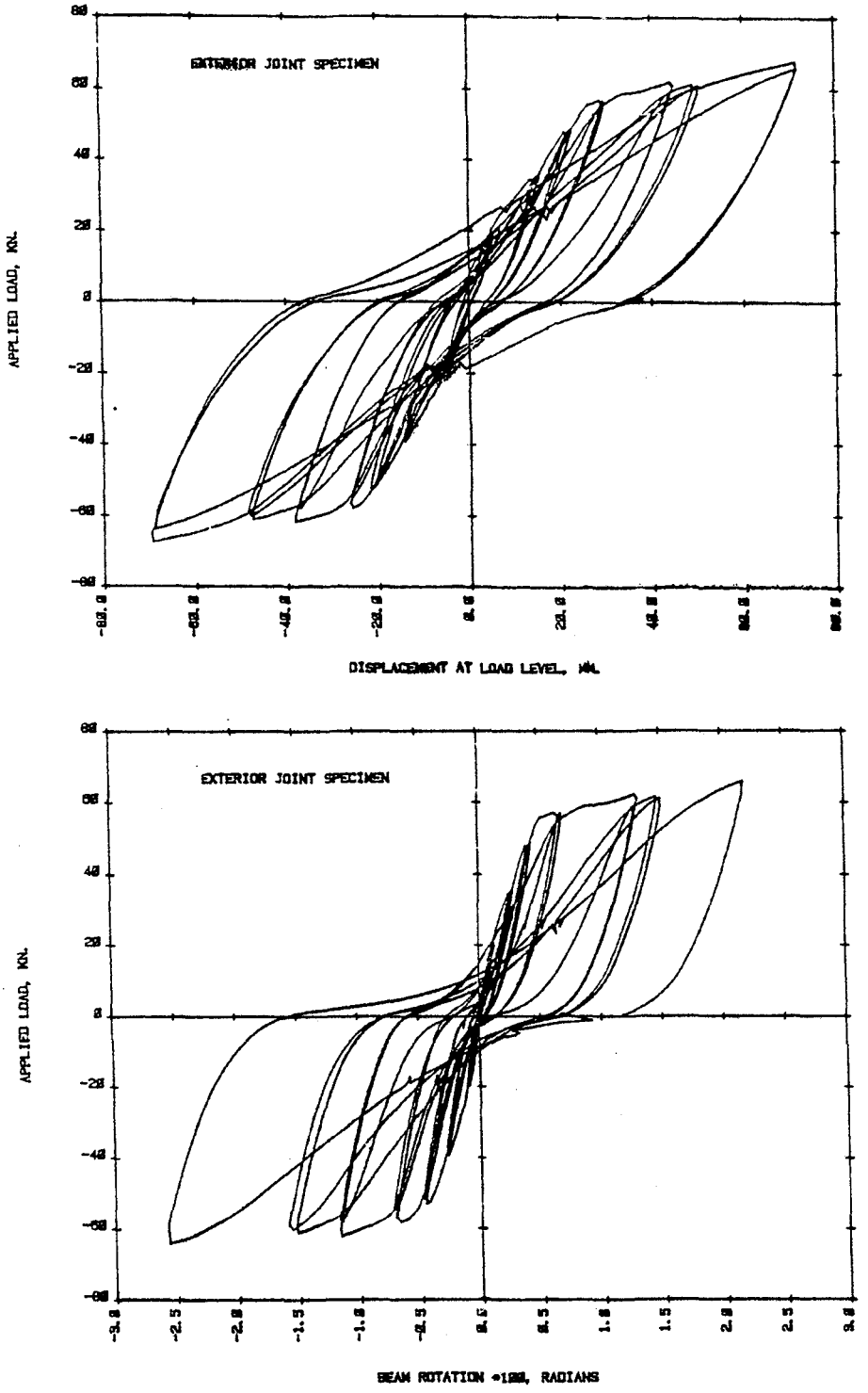

Fig. 3.2 Response of Exterior Joint

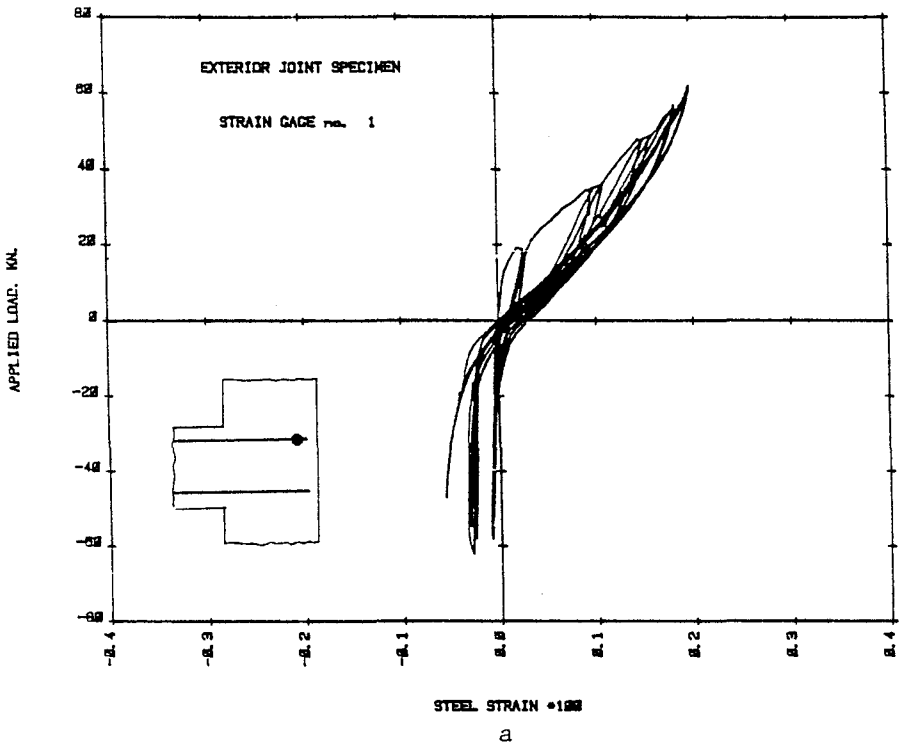

a

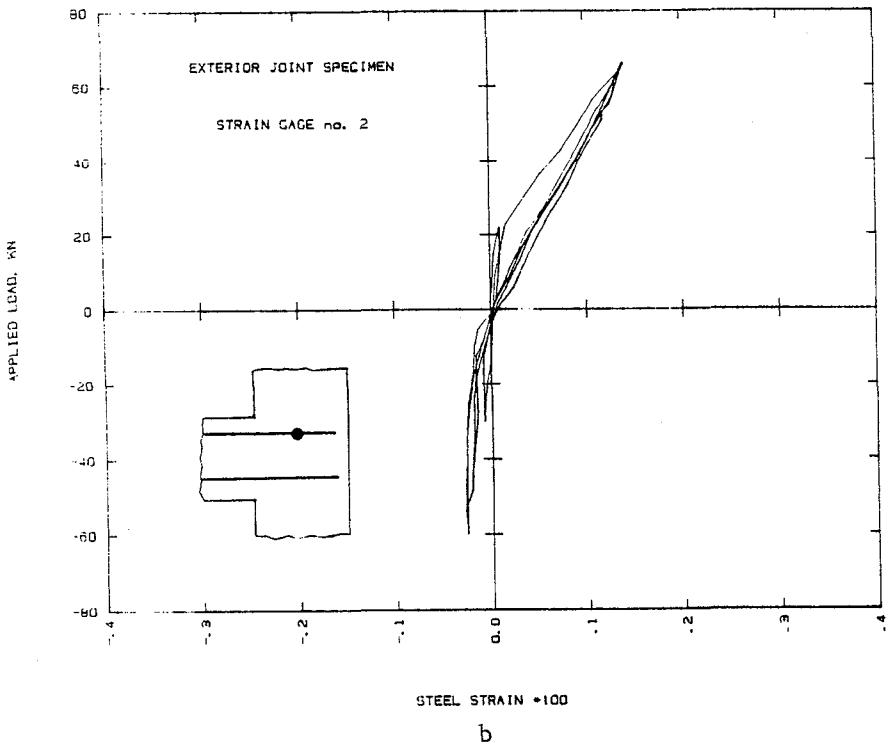

b

Fig. 3.3 Load-Strain Response for Exterior Joint

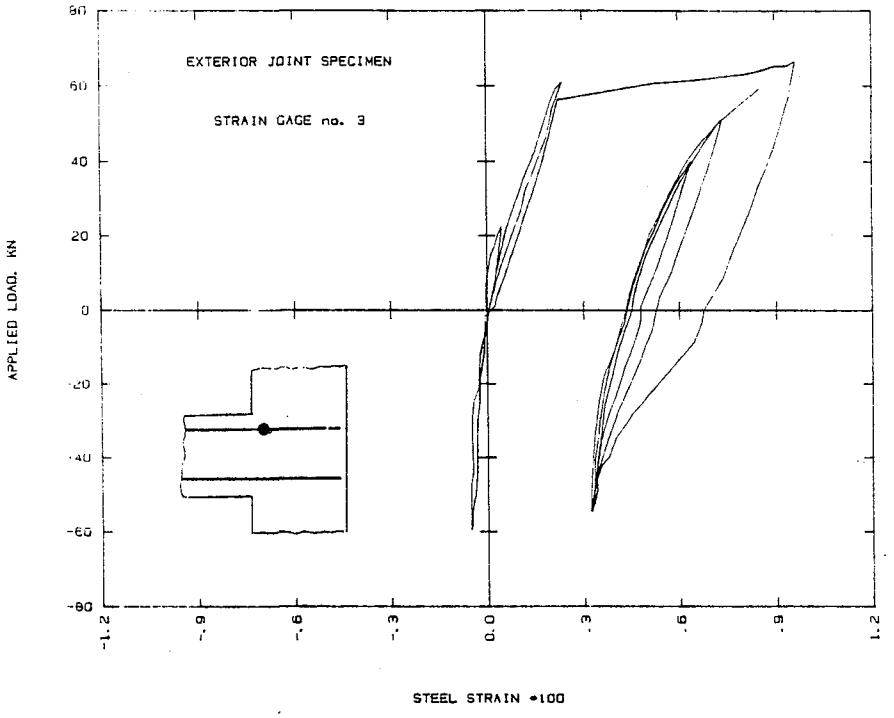

c

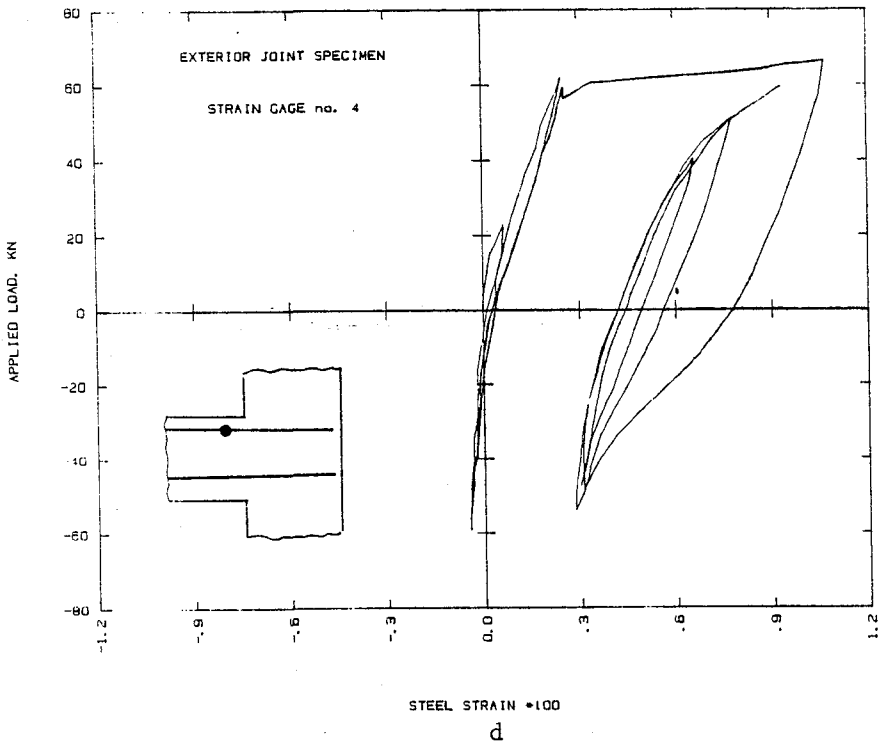

d

Fig. 3.3 Load-Strain Response for Exterior Joint

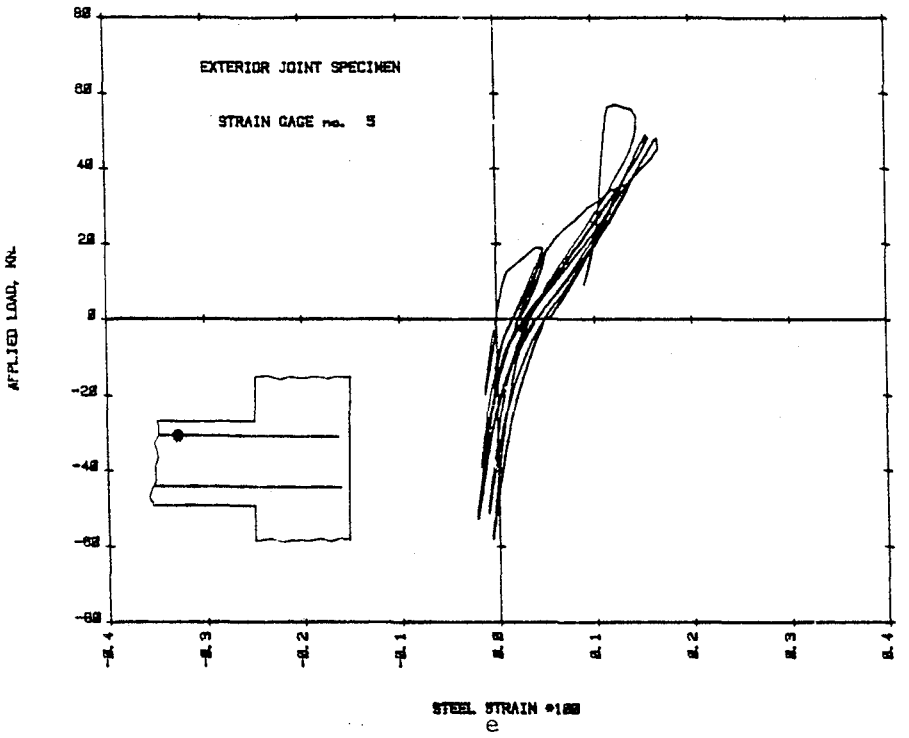

e

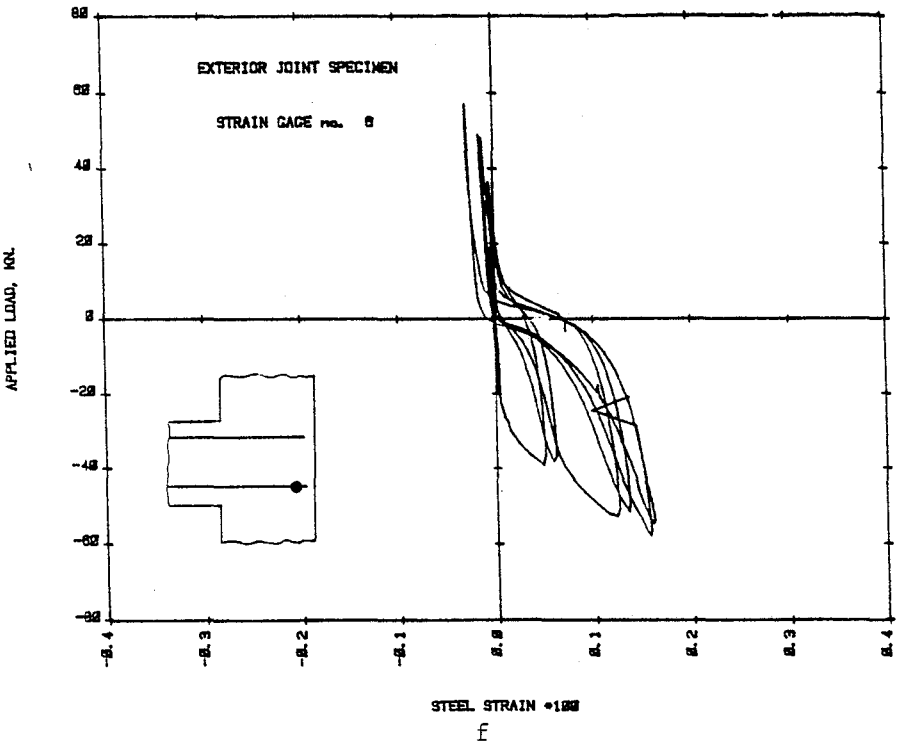

f

Fig. 3.3 Load-Strain Response for Exterior Joint

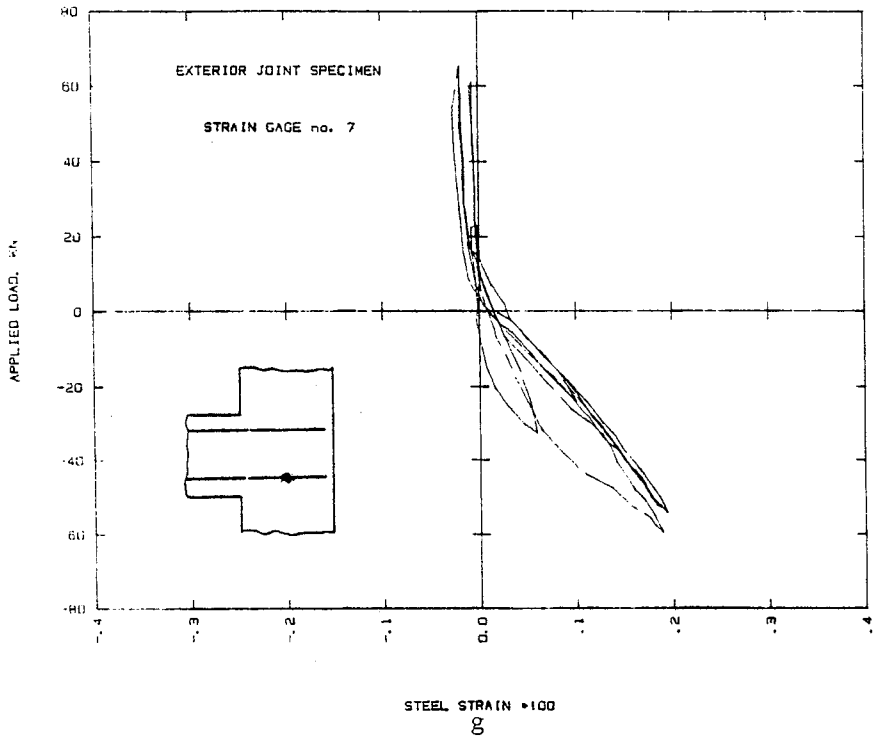

g

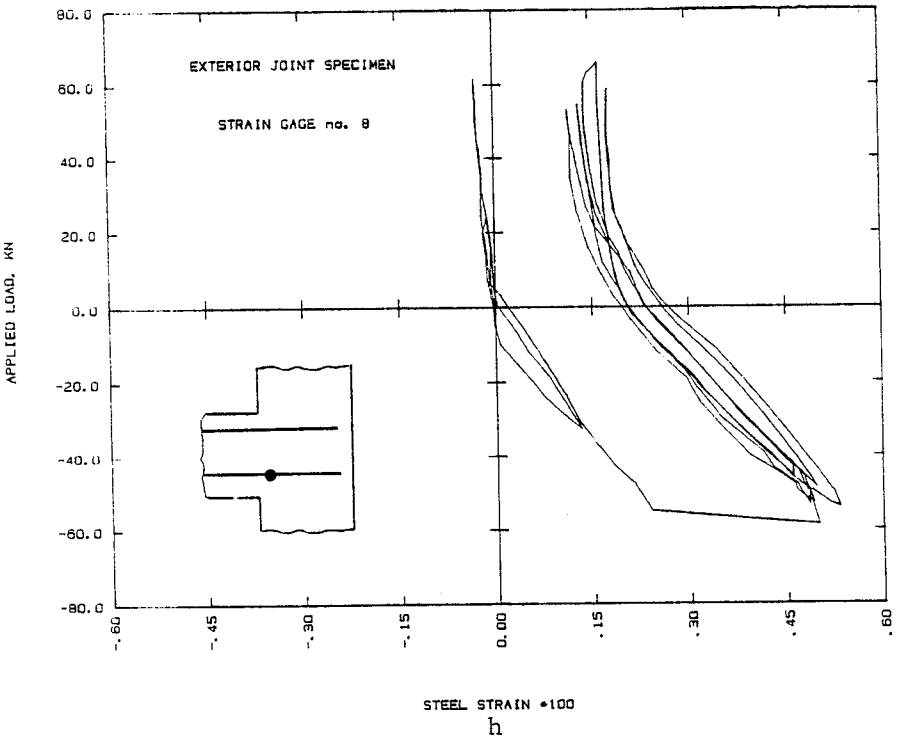

h

Fig. 3.3 Load-Strain Response for Exterior Joint

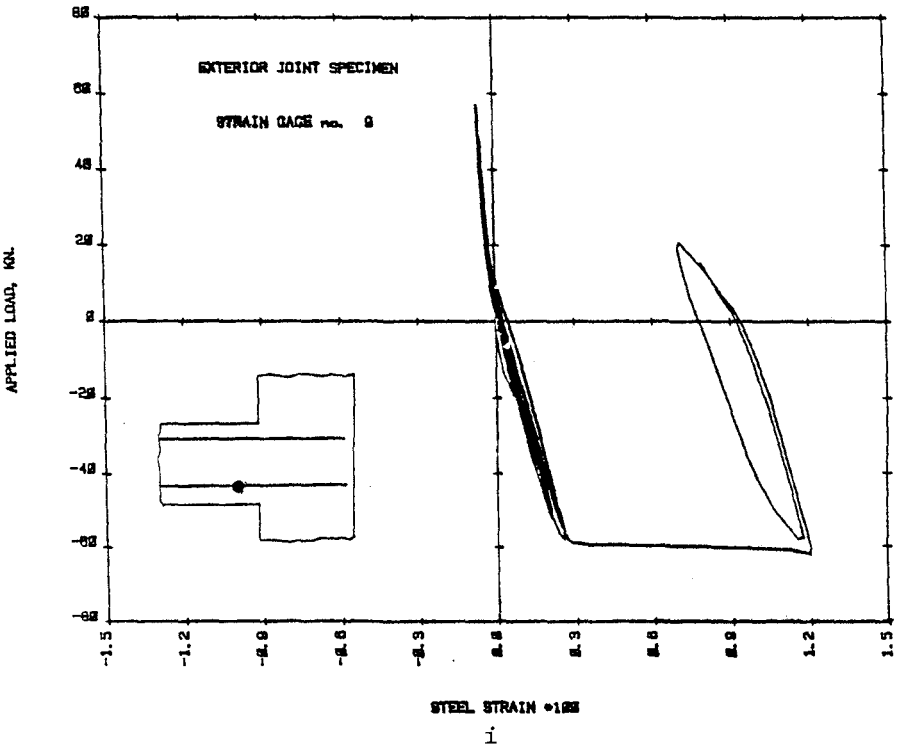

Fig. 3.3 Load-Strain Response for Exterior Joint

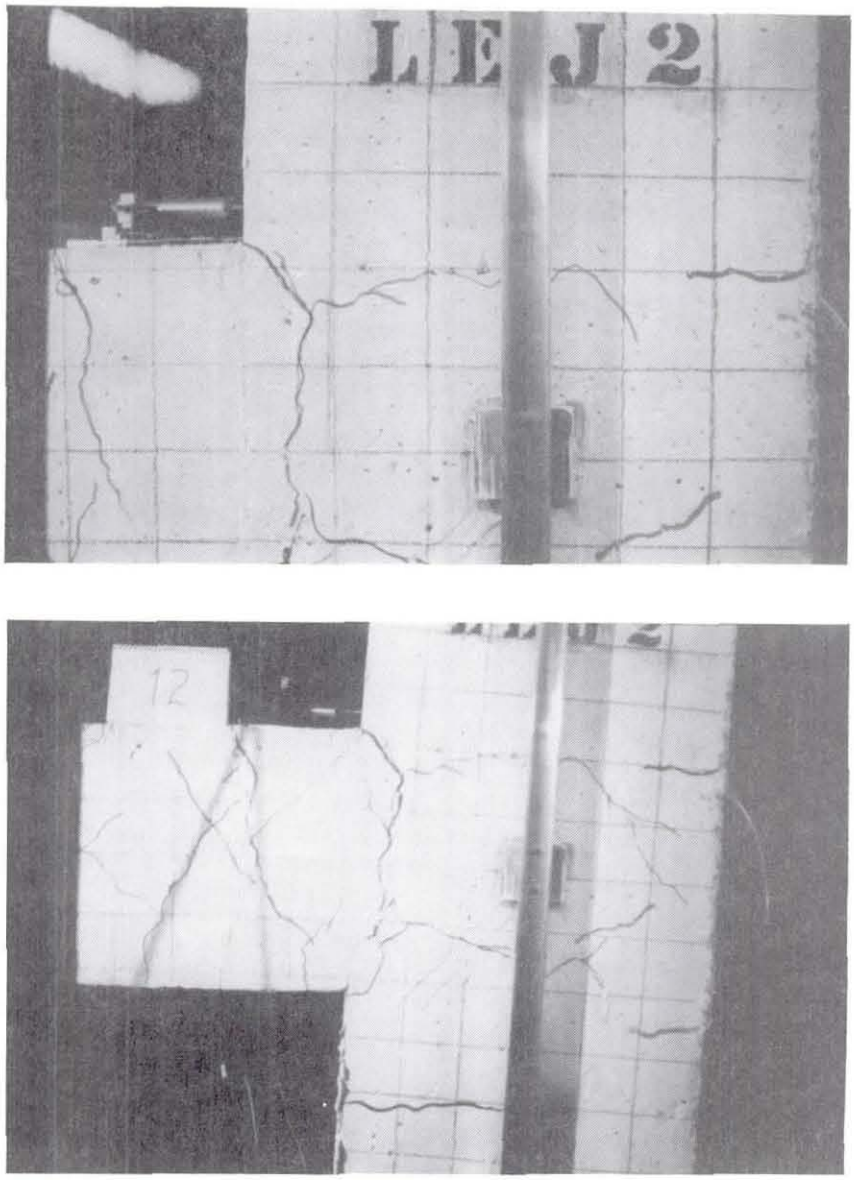

Fig. 3.4 Photographs of Damage of Exterior Joint

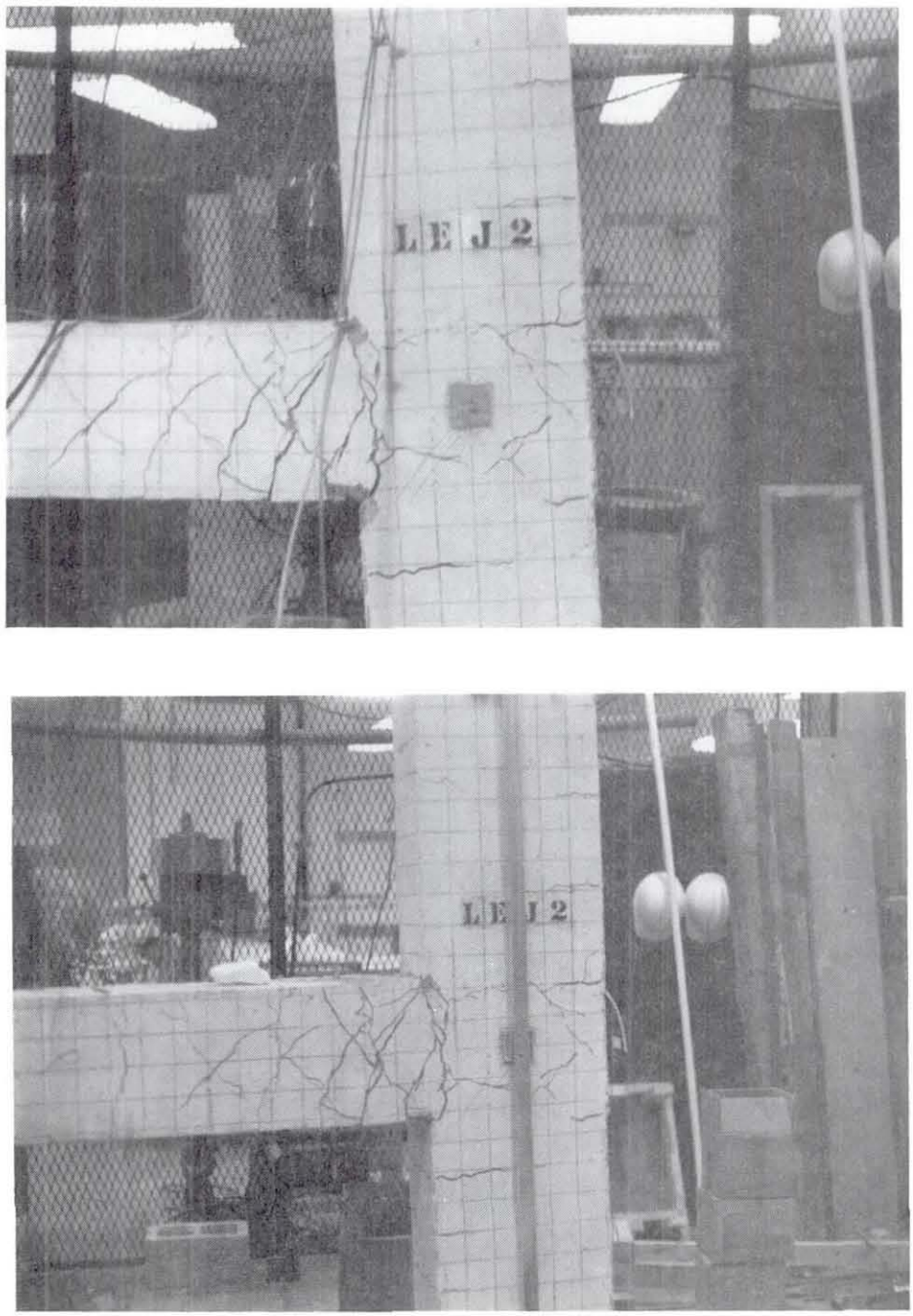

Fig. 3.4 Photographs of Damage of Exterior Joint

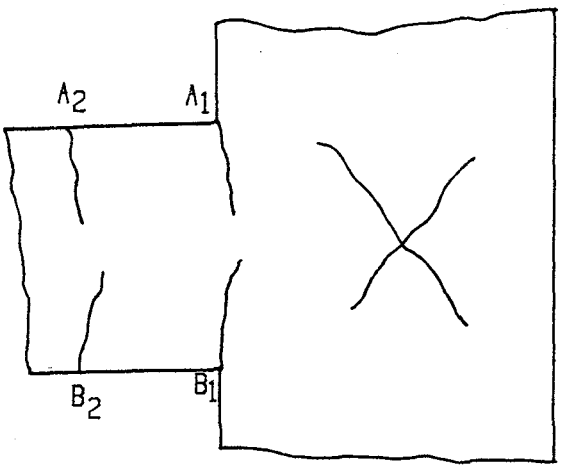

Cycle	A_1	A_2	B_1	B_2
5	.8		.8	
6	1.0		.9	
7	1.6		1.6	
8	1.8	.2	2.0	.2
9	2.5	1.0	2.5	.8
10	3.0	1.6	3.0	1.6
11	3.5	1.6	3.0	1.4
12	5.0	2.0	3.0	1.4
13	5.0	2.5	3.5	1.6
14	5.0	3.0	5.0	2.5
15	5.0	3.0	5.0	2.5

Fig. 3.5 Crack Widths for Exterior Joint

replication of the response between specimens was quite good. The following description of the characteristics response of the large-scale specimen was made in reference to the load-joint rotation relationship shown in Fig. 3.1.

As seen in Fig. 3.1a, the response to initial loading showed a high elastic stiffness up to point A, which was at 20 kN (4.5 kips). At this point the first flexural cracks opened, which caused the stiffness reduction seen in the response curve. This stiffness reduction was also seen in the load-strain curves in Figs. 3.3. During unloading the stiffness matched the original elastic stiffness. Loading in the opposite direction produced an identical response; a high elastic stiffness up to cracking at point B, a slight reduction in stiffness until unloading began, and a high unloading stiffness back through zero load.

The remaining five cycles shown in Fig. 3.1a represent all those in the pre-yield range of loading. During each successive cycle the loading stiffness decreased from the previous cycle. This was due to progressive cracking of the specimen, as shown by Figs. 3.4 and 3.5. Unloading stiffness remained high, but by the sixth cycle a noticeable stiffness reduction occurred near the loading axis at point C. At this stage, the original flexural cracks had opened wide enough so a crack on the top of the beam could not close before a crack on the bottom of the beam began to open. This left very little of the beam actually in contact with the column and created, momentarily, a soft section. The stiffness increased starting at point D in Fig. 3.1a because the cracks in the top of

the beam were then able to close. This was supported by the load-strain relationships in Figs. 3.3a and b which showed no increase in compressive strain upon further loading.

The eight curves shown in Fig. 3.1b represent the response in the post yield range of loading. When the load reached 58 kN (13 kips) at point E, yield occurred. This was evidenced by the load-strain curves in Fig. 3.3. Yielding caused the stiffness reduction seen after point E. In this range the unloading stiffness again started out very high, but the stiffness reduction near the load axis became more pronounced. In the last two cycles, cracking was so extensive that by the time the top cracks were able to close, the bottom cracks had opened far enough to prevent a noticeable increase in stiffness. The load-strain relationships in Fig. 3.3c and d showed a considerable change in compressive strain in later cycles which was caused by open flexural cracks. The particularly low stiffness along segment FG in the final cycle could have been due to a slight deterioration in bond. However, since the bars were anchored securely with a 90 degree bend, this effect of bar slip was minimal in the exterior joint.

Other general observations resulting from testing the exterior joints were as follows:

1) The shapes of the load-rotation and load-displacement curves were essentially the same. This indicated the deformations of the column were nearly elastic during the test.

2) The shapes of the load versus joint rotation and load versus beam rotation curves were similar, which indicated that most

of the nonlinear action of the beam occurred at the column face. Furthermore the beam rotations were a significant amount of the total rotations, which suggested nonlinear behavior in the joint region.

3) The strength of each specimen did not deteriorate with cycles of large deformation.

4) If a new maximum rotation was not reached during the current cycle, there was little reduction in stiffness upon loading.

5) If during the current cycle, the specimen was loaded to no more than the maximum load of the preceeding cycle, there was a reduction in the area bounded by the hysteresis loop. This represented a decrease in the amount of energy dissipated which was a result of increased deformations within the joint region.

6) Each specimen's ability to deform exceed the stroke length of the loading actuator (+-5 inches). In no case did a crushing failure or reinforcement fracture occur.

3.3 Comparison of Large and Small-Scale Specimens

For comparison purposes the load-rotation curve for the large-scale specimens was reproduced in Fig. 3.6 along with a similar curve for the small-scale specimens. In this figure the vertical axis for the small-scale specimens was normalized to increase the flexural strength for direct comparison with the response of the large-scale specimen. The adjustment factor was the square of the length scale factor (9) multiplied by the ratio of the products of the reinforcing ratio and the measured yield load:

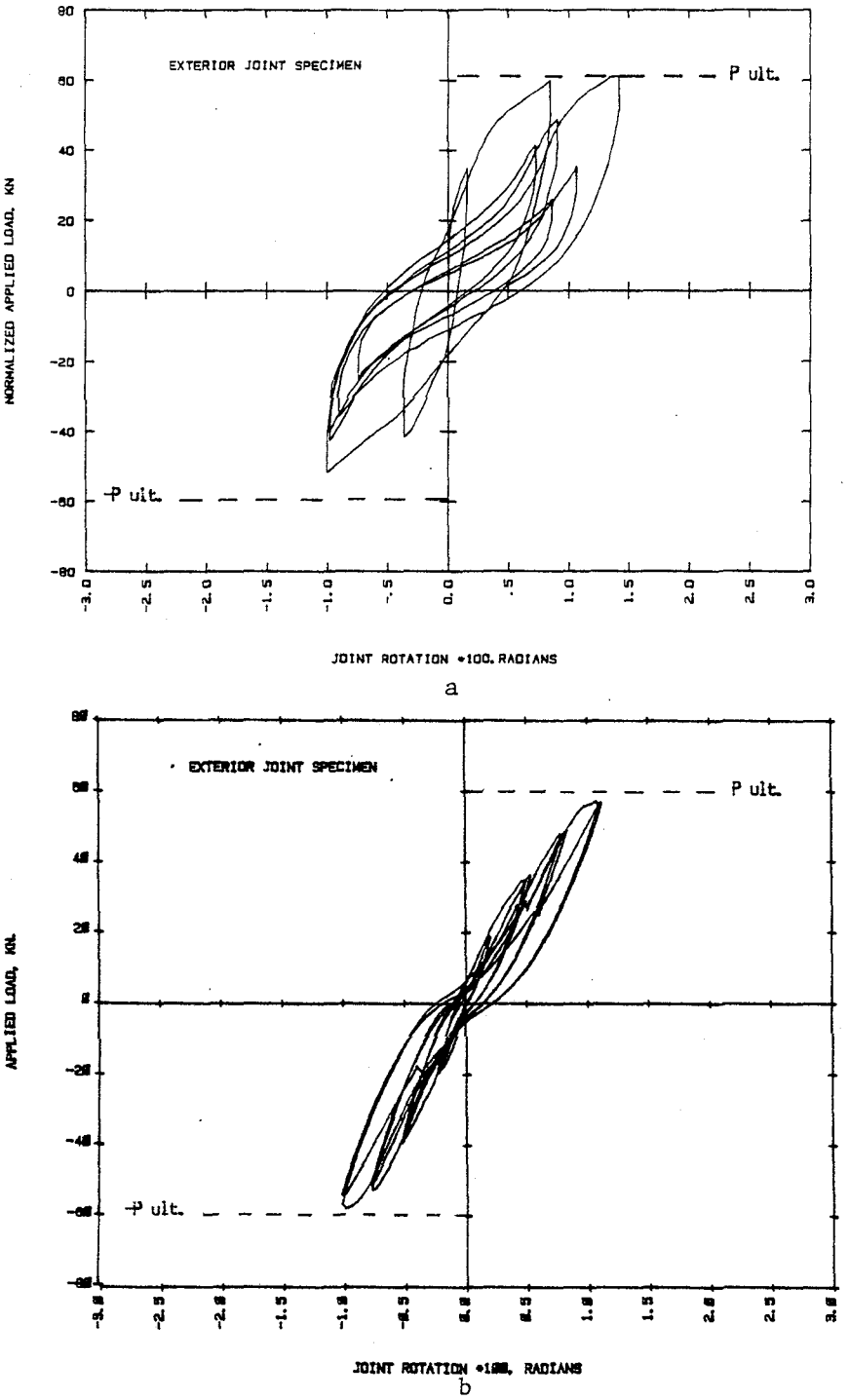

Fig. 3.6 Comparison of (a) Small-Scale and (b) Large-Scale Specimens

$$P_{LS} = \lambda^2 \frac{(\rho f y_{LS})}{(\rho f y_{SS})} P_{SS}$$

Conventional principles of mechanics assumed for ultimate strength design were used to determine this scaling factor. The horizontal axis, rotation, was nondimensional and therefore not adjusted.

Within the range of rotation of +-.010 radians, the stiffness characteristics exhibited by the large-scale specimens were modeled well by the small-scale specimens. The response of the small-scale specimens showed similar trends to the response of the large-scale specimens with regard to stiffness reduction at first cracking, a gradual degradation of stiffness upon loading, and a high unloading stiffness which reduced near zero load. The small-scale specimens also modeled the slight stiffness increase upon loading representing crack closure. One further similarity was that no substantial loading stiffness reduction occurred in cycles which did not contain new extreme rotations.

When looked at qualitatively, the two figures in Fig. 3.6 gave further information regarding the effects of scaling on strength and stiffness. A normalized cracking load of about 30 kN (6.75 kips) was observed for the small-scale specimens. This was somewhat higher than that of the large-scale specimens. This may have been attributable to a higher strength in the mortar from which the small-scale specimens were cast. The normalized maximum load of the small-scale specimens was approximately 60 kN (13.5 kips) which matched that of the large-scale specimens.

In the load reversal region, the reduced stiffness segment extended through a rotation equal to approximately .010 radians for the small-scale specimens, as compared to approximately .005 radians for the large-scale specimens. This may have been attributable to bond deterioration which was more prevalent in all of the small-scale specimens tested. The relatively weaker bond resulted in the lower average stiffness of a complete cycle for small-scale specimens.

The weaker bond resistance of the small-scale specimen may be inferred by the change of slope of the load-rotation curve (Fig. 3.6a). During the first large amplitude cycle, in the first quadrant of loading, a significant change of stiffness was observed after cracking but before yield of reinforcement should have occurred. It should also be noted that no appreciable cracking had occurred due to diagonal tension within the joint of the specimen. This change of slope may have been attributable to a localized deterioration in bonding of beam reinforcement within the column. During subsequent cycles of loading, the stiffness in this range was greatly reduced. This tendency was also observed during the third cycle following the first large amplitude cycle.

Because of the limited range of the response of the small-scale specimens, direct comparisons with the large-scale specimens could not be made for rotations greater than .010 radians. However, as previously mentioned, specimens at both scales resisted nearly equal loads at maximum rotations. These loads were slightly less than loads calculated by conventional mechanics used

in ultimate strength design (16) which have been shown in the figure. In addition, the unloading slopes during large amplitude cycles were very similar for specimens at both scales. These similarities suggest that the large-scale specimens' behavior could be represented well by the small-scale specimens for loading cycles in the non-linear, or post-yield, range of response.

CHAPTER 4

SCALE RELATIONSHIPS OF INTERIOR JOINTS

4.1 Introduction

This chapter is a description of how accurately small-(1/12) and medium-(1/4) scale interior joints models could predict the response of large-scale prototypes. As with the exterior joints, the large-scale specimen was considered the control, and its response is explained in detail. A brief description of the fourth large-scale specimen follows, pointing out the differences in response due to a different distribution of longitudinal reinforcement. Then the small, and finally the medium-scale specimen responses are compared to that of the large-scale specimen.

4.2 Description of the Large-Scale Specimen Response

The load-rotation curve representing the first three large-scale specimens is shown in Fig. 4.1. The load-displacement, load-beam rotation, and load-strain relationships are plotted in Figs. 4.2-4.4. Photographs of damage and crack information are presented in Figs. 4.5 and 4.6. Data is presented for just one specimen because replication with other specimens was very good. The characteristic response is described with reference to the load-rotation response of Fig. 4.1.

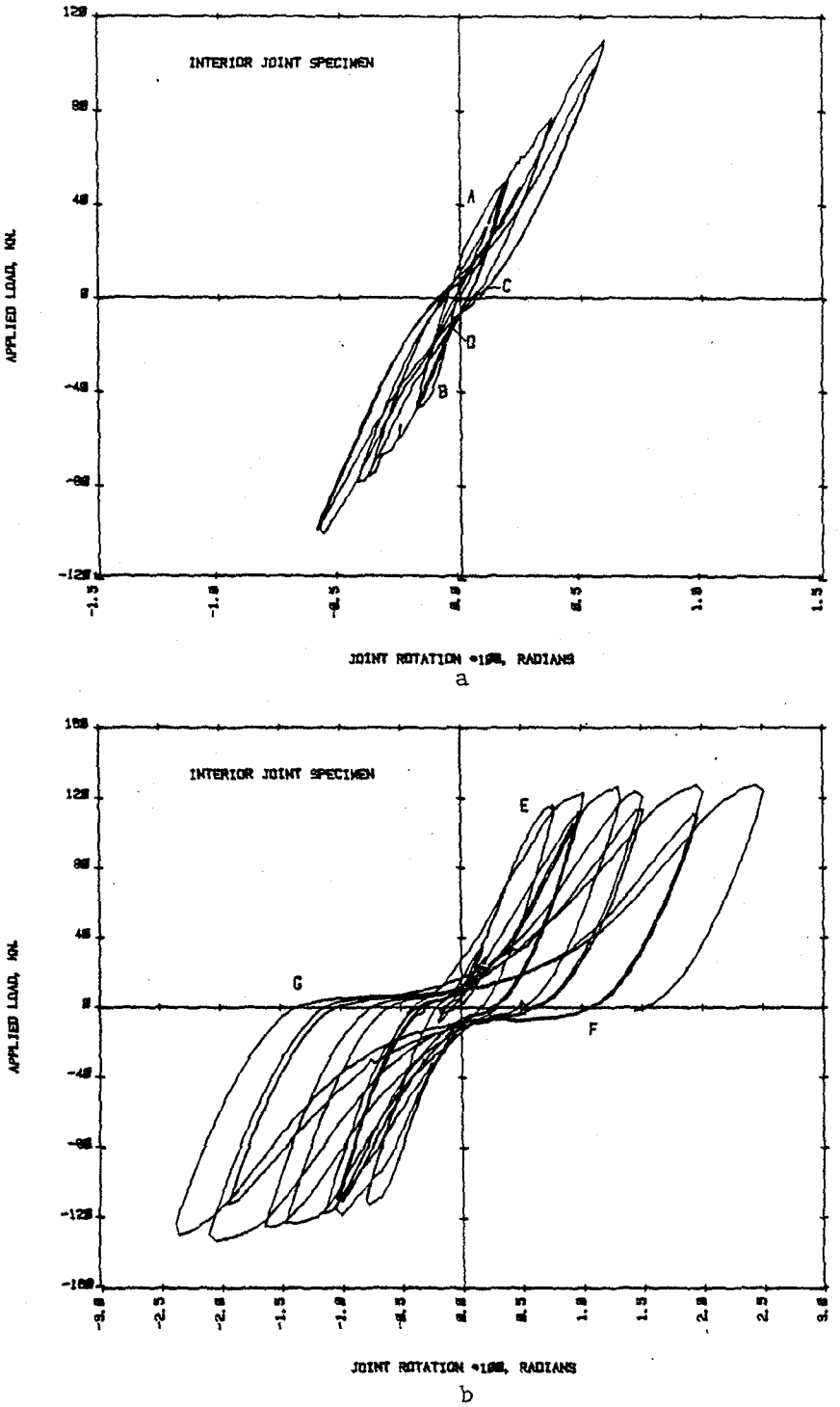

Fig. 4.1 Load-Rotation Response for Interior Joint

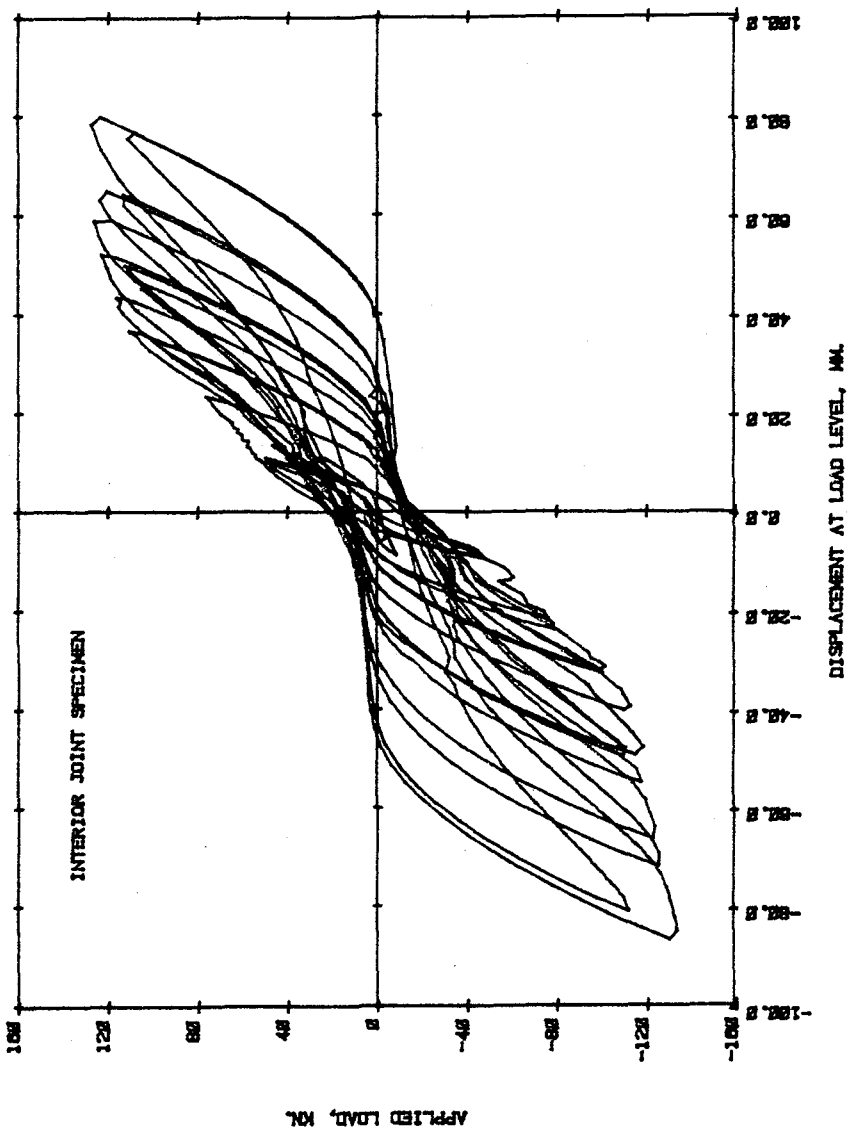

Fig. 4.2 Load-Displacement Response for Interior Joint

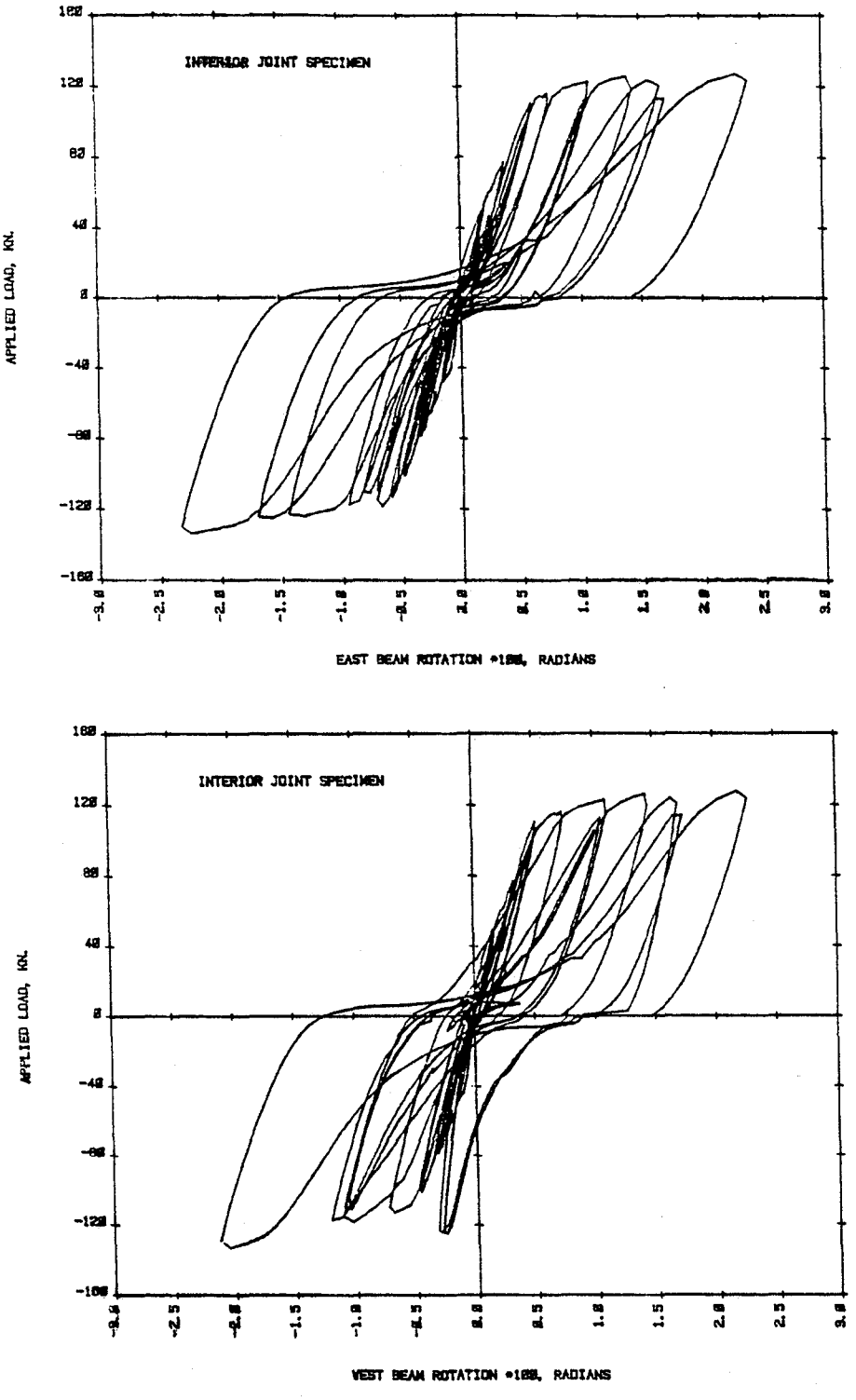

Fig. 4.3 Measured Beam Rotations in Interior Joint

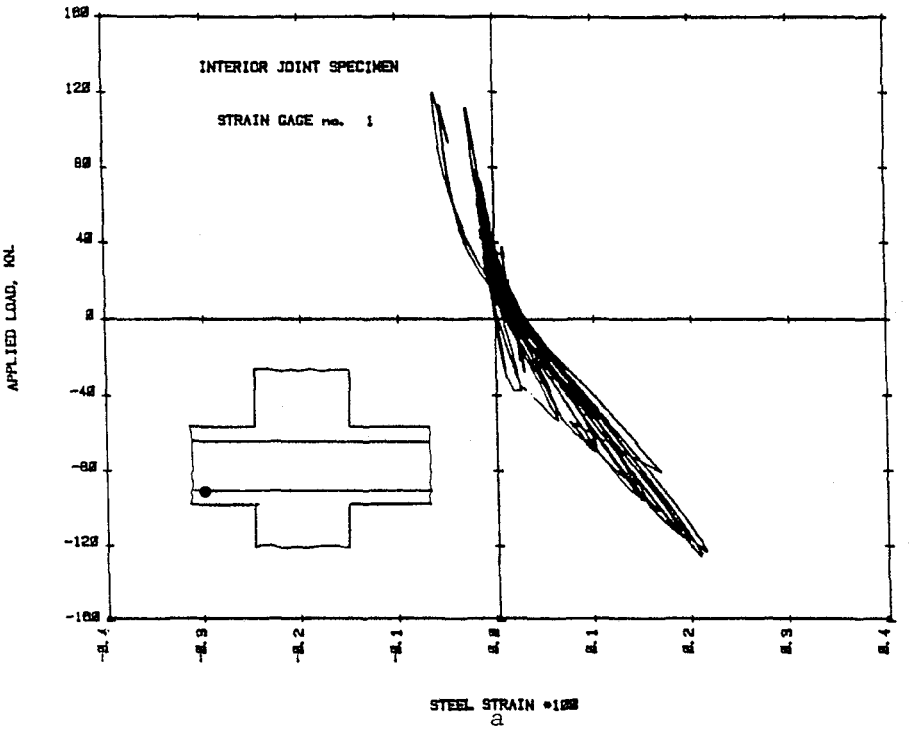

a

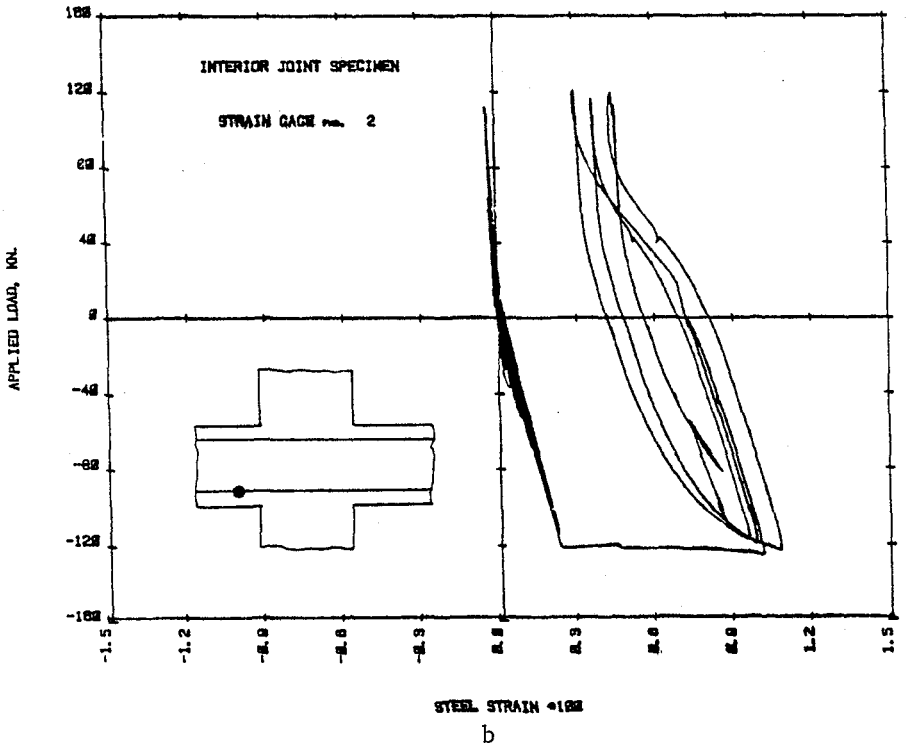

b

Fig. 4.4 Load-Strain Response for Interior Joint

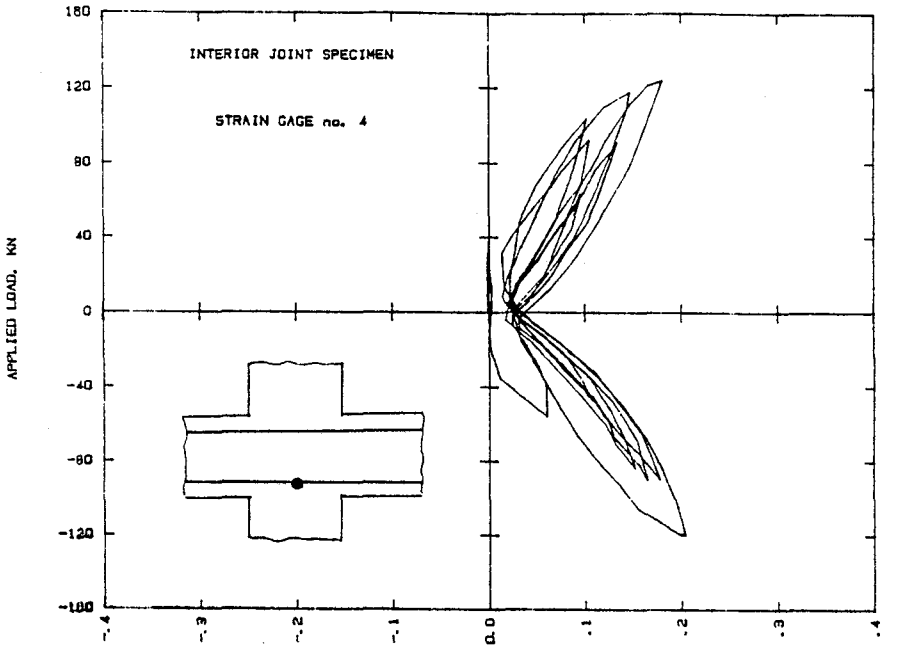

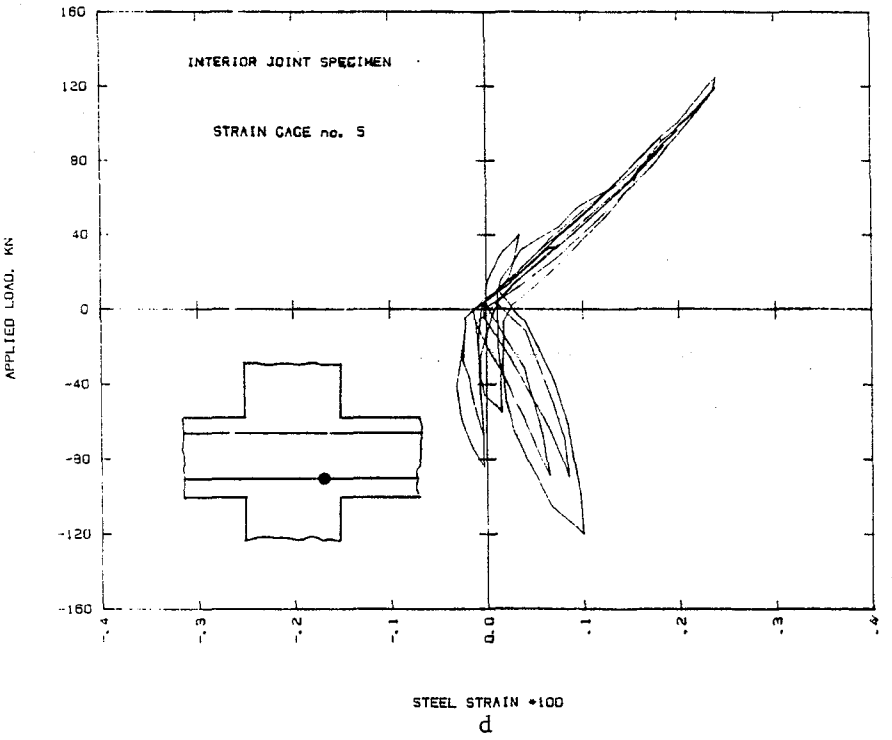

Fig. 4.4 Load-Strain Response for Interior Joint

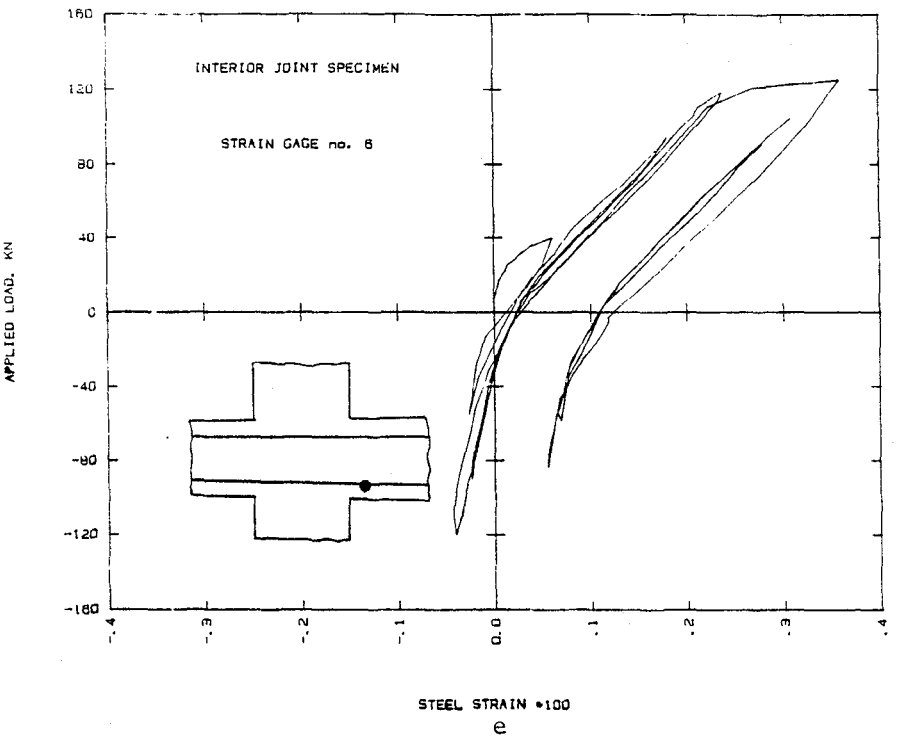

e

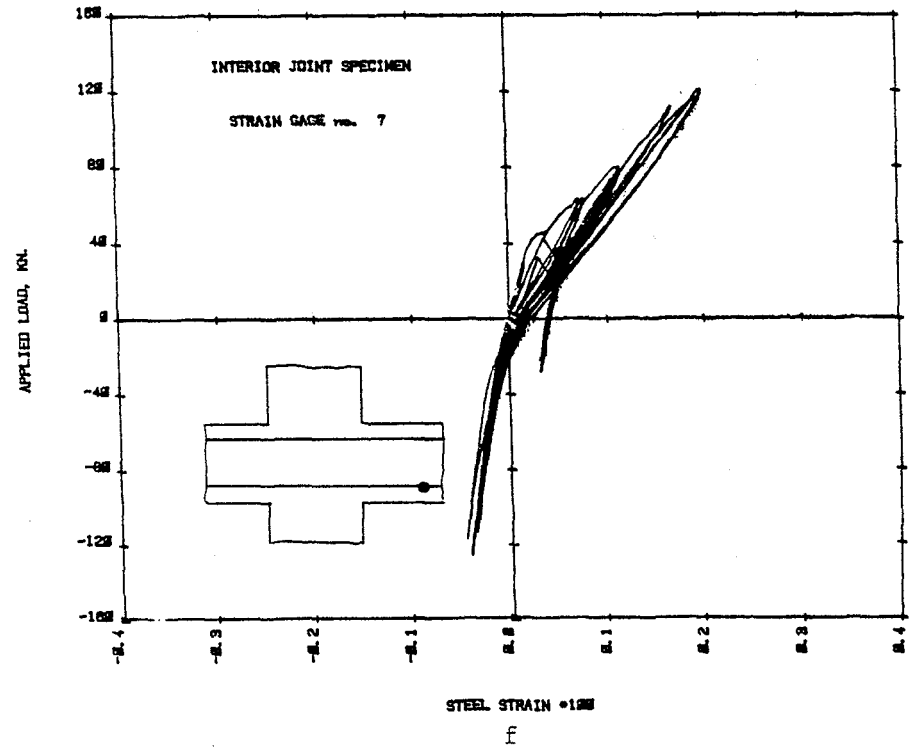

f

Fig. 4.4 Load-Strain Response for Interior Joint

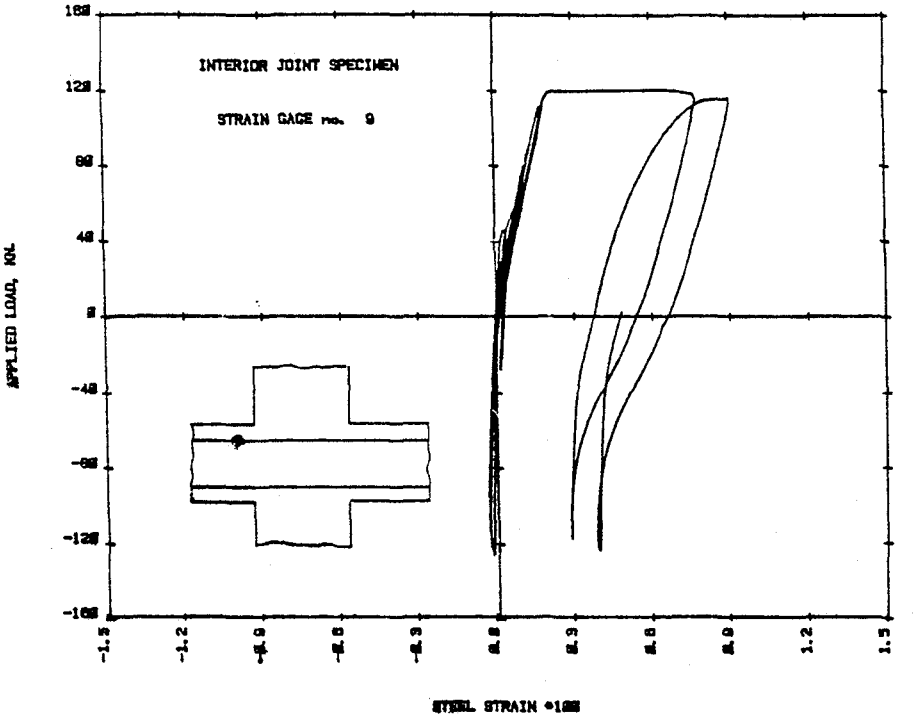

g

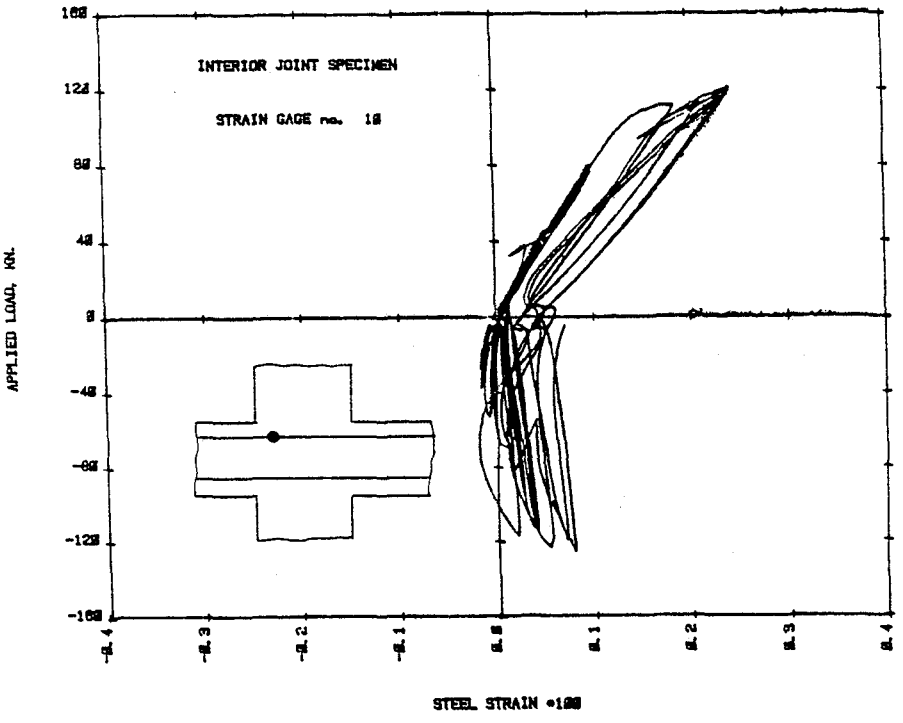

h

Fig. 4.4 Load-Strain Response for Interior Joint

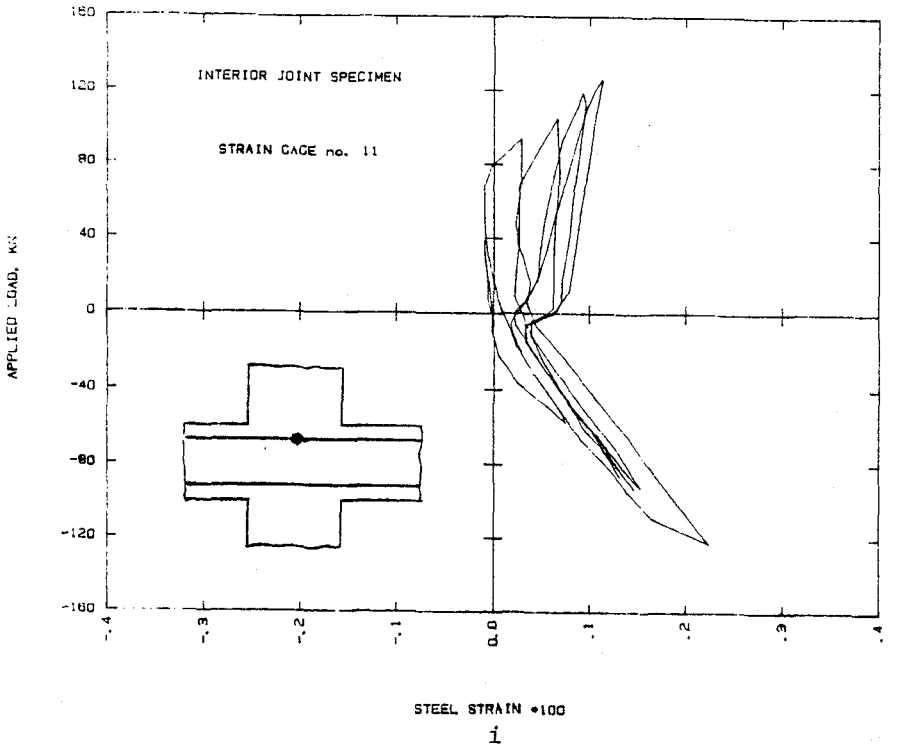

i

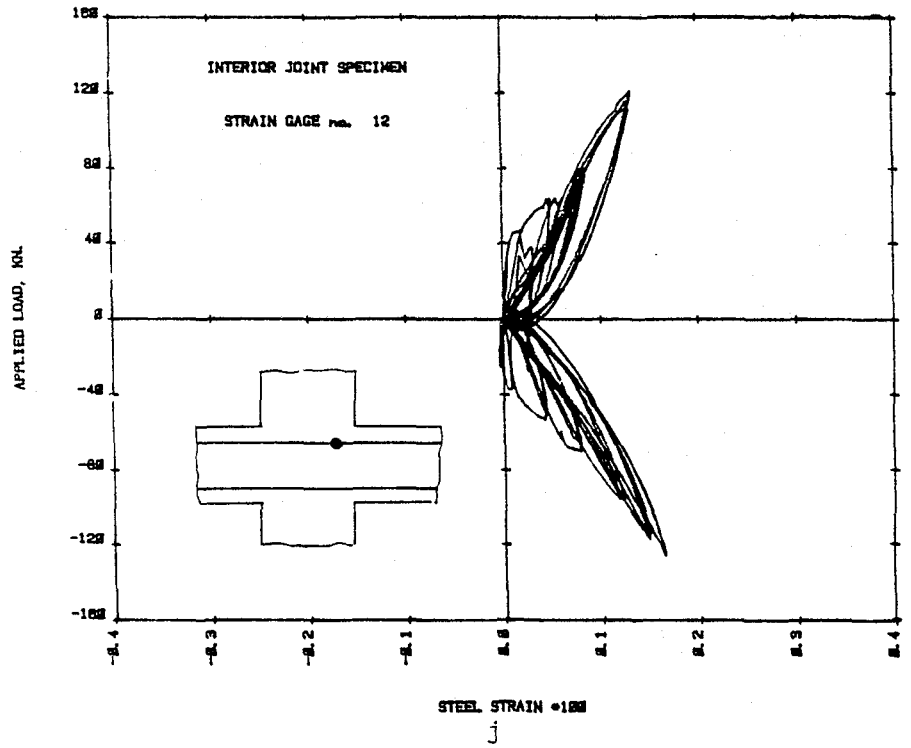

j

Fig. 4.4 Load-Strain Response for Interior Joint

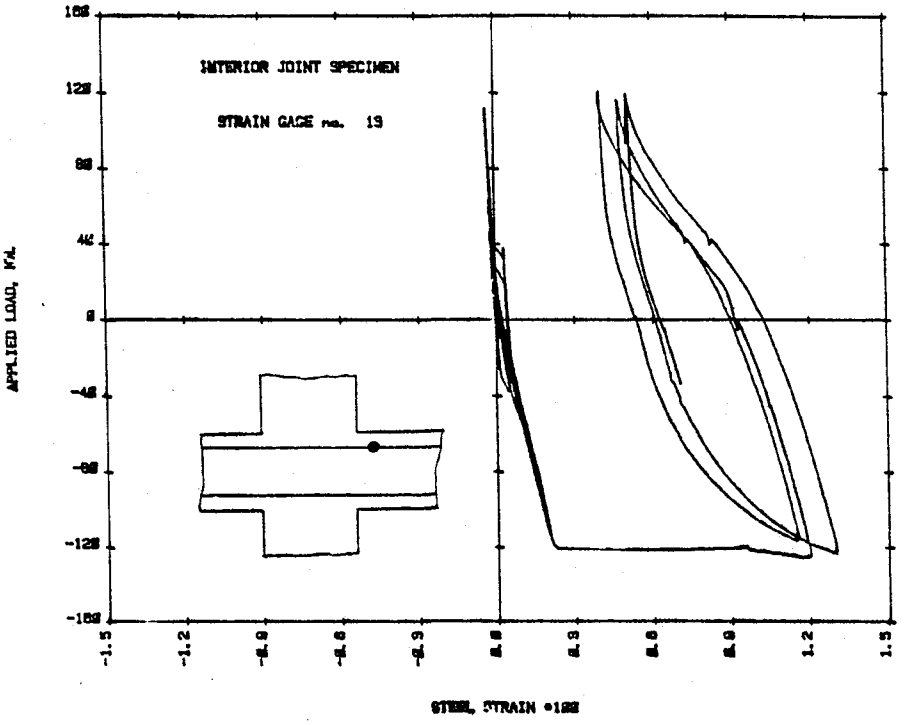

k

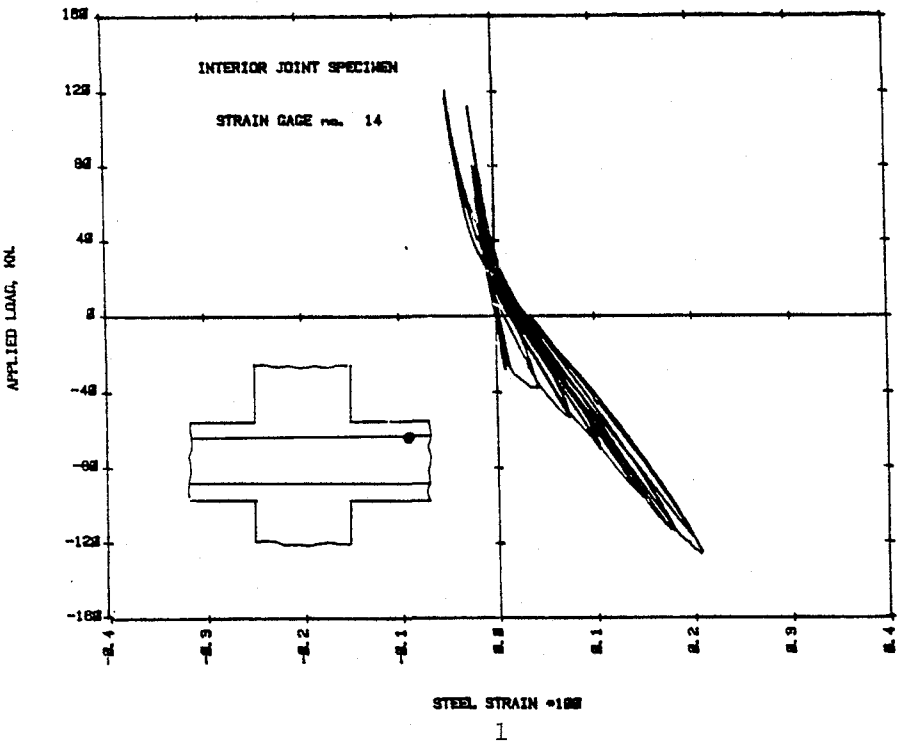

l

Fig. 4.4 Load-Strain Response for Interior Joint

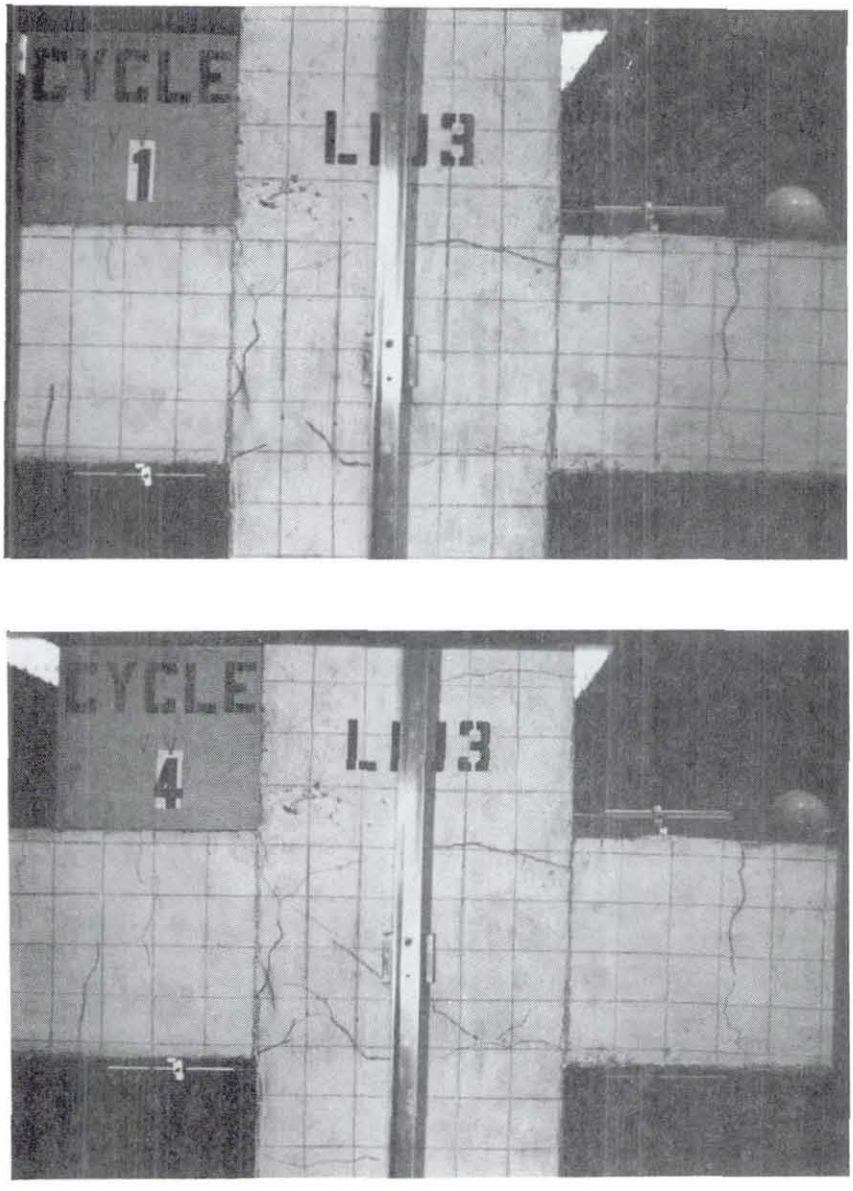

Fig. 4.5 Photographs of Damage of Interior Joint

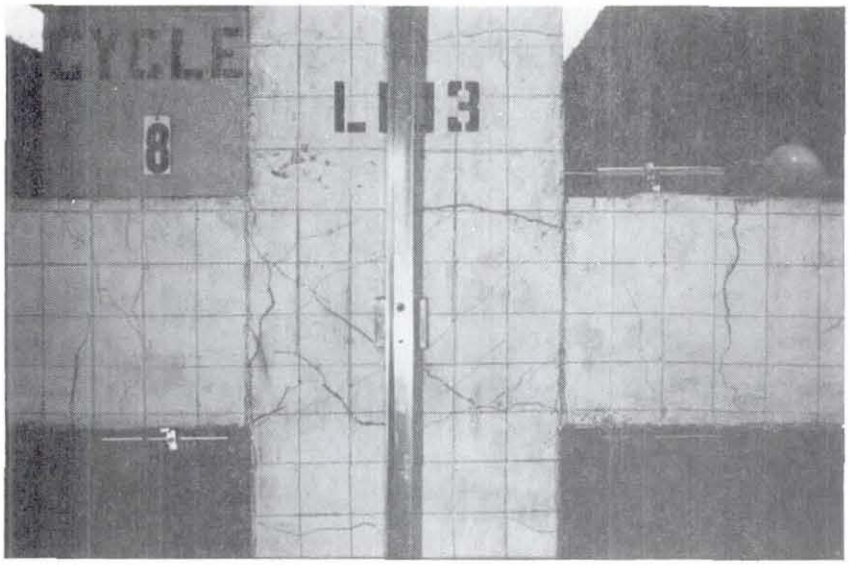

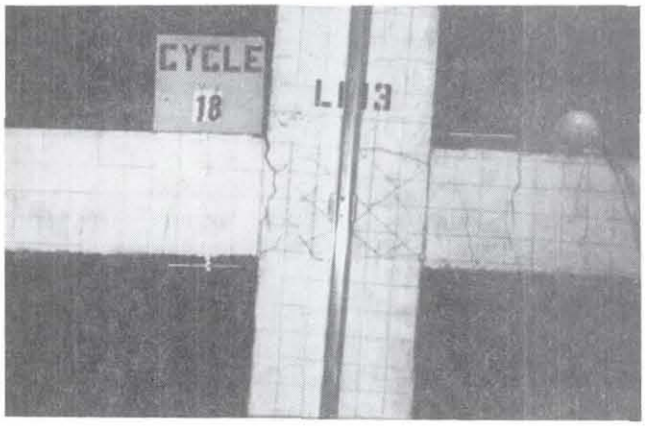

Fig. 4.5 Photographs of Damage of Interior Joint

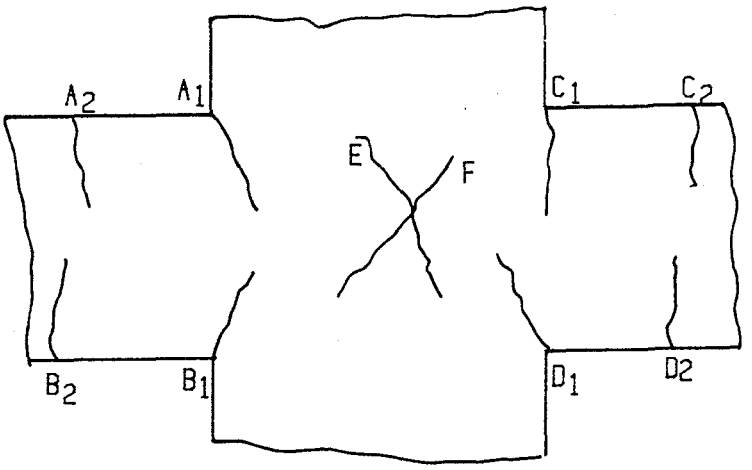

Cycle	A_1	A_2	B_1	B_2	C_1	C_2	D_1	D_2	E	F
4	.5		.3		.4	.3				
5	1.4		.5		1.4	.6	.6			
6	1.4	.2	.5	.2	.7	.3	.7			
7	2.0	.2	.5	.2	.7	.3	1.0			
8	2.0	.2	.7	.2	1.8	.6	1.0			
9	2.0	.2	1.4	.2	1.8	.4	1.0		.4	
10	3.0	.5	1.4	.2	1.8	.4	1.0		.6	.3
11	3.0	.5	1.4	.2	2.0	1.4	1.0		.6	.3
12	3.0	.5	1.4	.2	2.0	1.5	1.5		.6	.7
13	3.0	.5	2.5	.7	2.5	.6	1.5	.6	1.2	1.0
14	4.0	.6	3.5	.4	3.0	.4	2.5	1.6	1.2	1.0
15	5.0	1.4	4.5	1.0	5.0	.6	2.5	2.0	1.2	1.2

Fig. 4.6 Crack Widths for Interior Joint

Referring to Fig. 4.1a, the specimens responded to initial loading with a high elastic stiffness up to the cracking point A, which occurred at 40 kN (9 kips). Cracking caused a stiffness reduction which continued until the unloading point. This phenomena was also observed in the load-strain responses in Fig. 4.4. The unloading stiffness matched the loading stiffness. As was always the case, loading in the opposite direction produced an identical response: a high elastic stiffness reduced when cracks opened at point B. The reduced stiffness continued until unloading, upon which the stiffness assumed its high elastic value back through zero load.

The remaining five cycles shown in Fig. 4.1a represent all those in the pre-yield range of loading. The gradual decrease in loading stiffness was caused by progressive cracking in the specimens. Unloading stiffnesses continued to be high, but near the load reversal point (point C in Fig. 4.1a) a stiffness reduction became apparent. This was due partially to open flexural cracks on both faces of the beams, but more importantly, it was due to some deterioration of the steel-concrete bond within the joint region. Since the curve between points C and D had some slope, it indicated the specimens were resisting load. This suggested that the bond had not been completely destroyed. At point D, flexural cracks on beam faces A and D (Fig. 4.6) closed, thereby causing a stiffness increase.

The family of curves in Fig. 4.1b represents the response in the post-yield range of loading. Yield occurred at a load of 118 kN

(26.5 kips) as shown in by load-strain graphs in Fig. 4.4. Yield caused the stiffness reduction seen at point E on Fig. 4.1b. The response curves in this range showed the unloading stiffness to start out very high, but to gradually decrease as the curve approached zero load. In the load reversal region between points F and G, the stiffness was observed to decrease more and more. This was caused by progresive bond deterioration of the beam bars within the joint. By the final cycle the bond had been completely destroyed and the curve in that region was essentially horizontal. With no bond resistance, the tensile force in the beam bars was constant across the width of the joint. This phenomenon, coupled with the fact that no concrete was in compression because of open flexural cracks, caused the specimens to have no resistance to loading. The specimens could resist load only after the column had rotated far enough to close some of the flexural cracks and subject the concrete to flexural compressive stresses.

The progression of bond deterioration could also be inferred from the load-strain relationships. As more of the bond was destroyed, a longer segment of a bar was put into tension. Eventually, when the bond was completely destroyed, the segment of a bar within the joint region was constantly in tension. This was seen in Figs. 4.4c,d,h,i,j which were the responses indicated by all the strain gages within the joint.

4.3. Comparison of Large-Scale Interior and Exterior Joints

The six general characteristics listed at the end of Section 3.2 for exterior joints were also observed during the tests of interior joints. However, the two configurations showed two distinct differences in their responses. First, the interior joints resisted twice the load, at both cracking and yield, as did the exterior joints. This would be expected since the interior joints had two beams extending from them. The second difference was the exterior joints showed much less stiffness loss in the load reversal range of the response. This was because bond deterioration in the exterior joints was not nearly as great as in the interior joints.

4.4 Differences due to Different Reinforcement

The reader should recall the fourth large-scale interior joint specimen was reinforced differently from the first three. While the area of steel in the beams was kept essentially the same, smaller diameter bars were used. This section discusses the effect of that change. Fig. 4.7 shows the load-rotation relationship for this specimen. Photographs of damage and crack information are given in Figs. 4.8 and 4.9.

The effect of using smaller bars could be seen by comparing Figs. 4.7 and 4.1. For smaller bars (Fig. 4.7), the pinching of each hysteresis loop in the vicinity of the origin was not nearly as pronounced as for larger bars (Fig. 4.1). As discussed in Section 4.3, pinching of a hysteresis loop was an indication of slip of the beam reinforcement as a result of bond deterioration in the joint

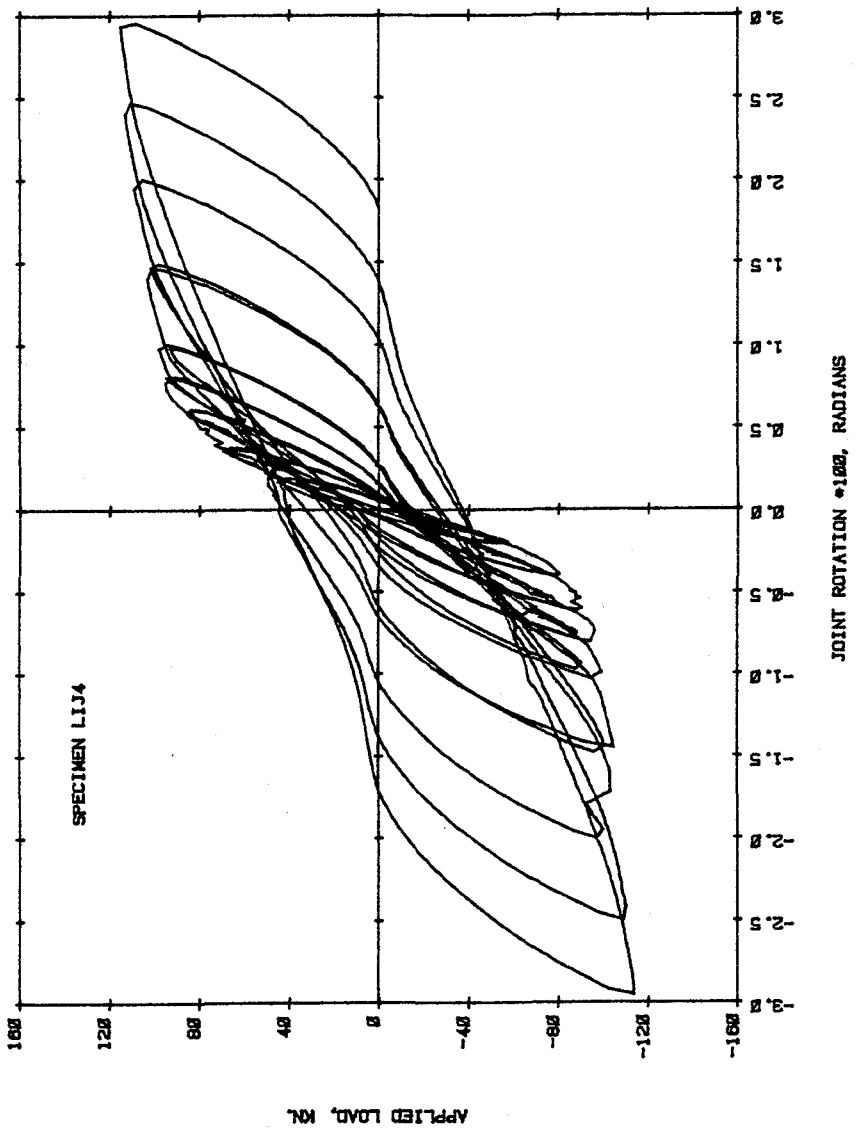

Fig. 4.7 Load-Rotation Response for Specimen LIJ4

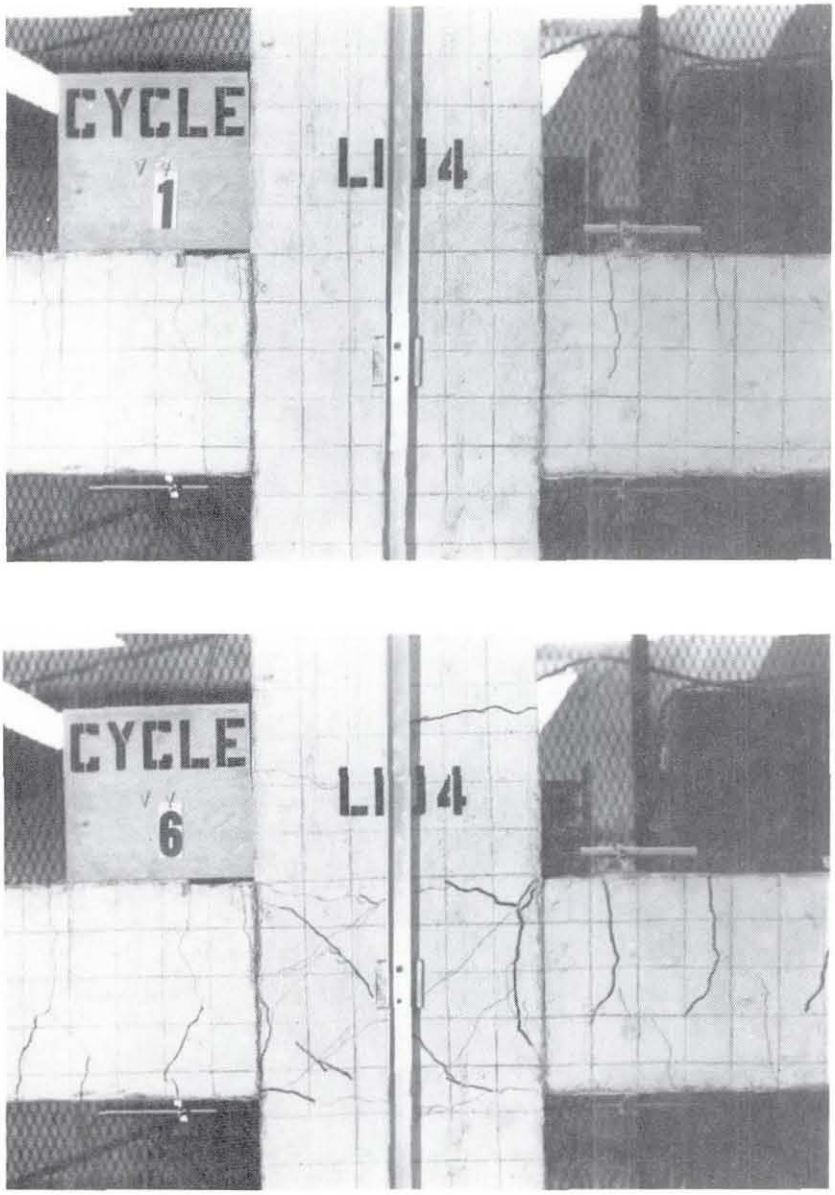

Fig. 4.8 Photographs of Damage of Specimen LIJ4

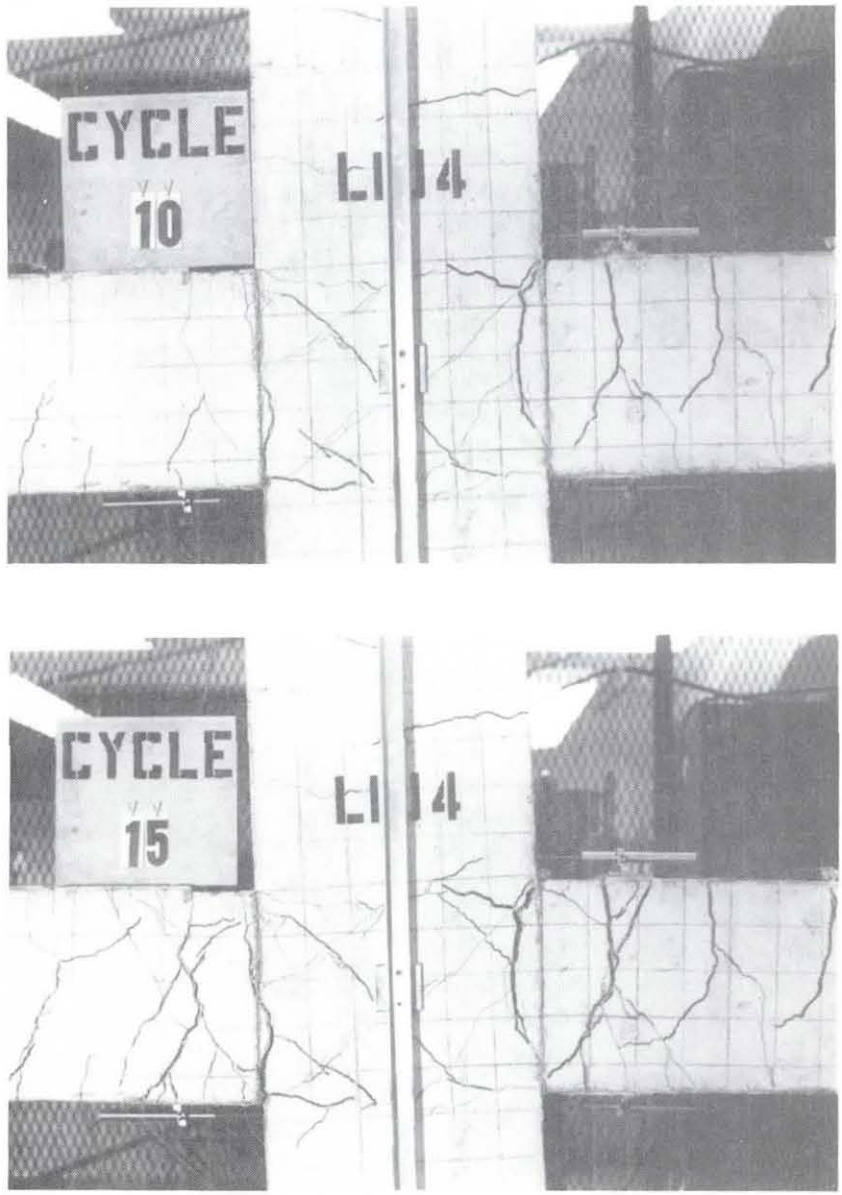

Fig. 4.8 Photographs of Damage of Specimen LIJ4

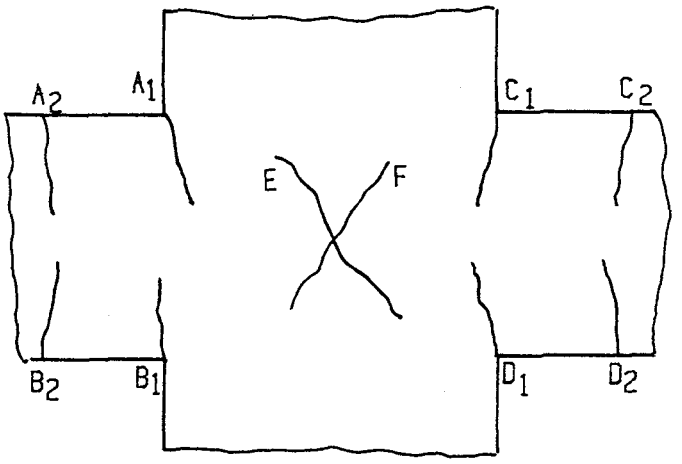

Cycle	A_1	A_2	B_1	B_2	C_1	C_2	D_1	D_2	E	F
3	.2	.2	.5	.2	.5	.2	.2	.2		
4	.4	.2	.6	.2	.6	.2	.4	.2	.2	.5
5	.7	.6	1.2	.4	1.2	.4	.7	.6	.2	.5
6	.9	.4	1.6	.5	1.6	.5	.9	.4	.4	.5
7	1.6	.9	2.5	.5	2.5	.5	1.6	.9	.4	.5
8	1.4	.5	3.0	.5	3.0	.5	1.4	.5	.3	.6
9	1.6	1.0	3.5	1.8	3.5	1.8	1.6	1.0	.3	.6
10	2.0	.9	3.5	1.0	3.5	1.0	2.0	.9	.5	1.0
11	2.5	1.8	4.0	3.5	4.0	3.5	2.5	1.8	.4	.8
12	3.0	1.8	4.0	3.5	4.0	3.5	3.0	1.8	.5	.8
13	3.5	2.5	4.5	5.0	4.5	5.0	3.5	2.5	.6	1.0

Fig. 4.9 Crack Widths for Specimen LIJ4

region. The load-rotation curve (Fig. 4.7) suggested bond deterioration was not as prevalent in the fourth specimen as in the first three. The reason for this was the shorter development length of the smaller diameter bars in the fourth specimen. This enabled the steel to accept higher tensile forces before the bond was damaged. For this reason, in the future attention should be given to modeling the ratio of reinforcement development length to the width of the column.

Another effect of the shorter development length was that the steel yielded at a lower load of 100 kN (22.5 kips). Ultimately though, the fourth specimen exhibited essentially the same strength as the first three. During the final cycle, the loading stiffness had reduced to where no noticeable yield point could be defined. This could have been attributable to the Bauschinger effect in the steel, since by this point the steel had been loaded past its yield point several times.

Like the first three specimens, the fourth specimen showed an ability to deform which exceeded the range of the loading actuator. No crushing failure occurred, nor did the reinforcing steel ever fracture.

4.5 Comparison of Large and Small-Scale Specimens

For comparison purposes, the load-rotation curve of Fig. 4.1 was reproduced in Fig. 4.10 along with a similar curve from tests of small-scale specimens. In this figure the vertical axis

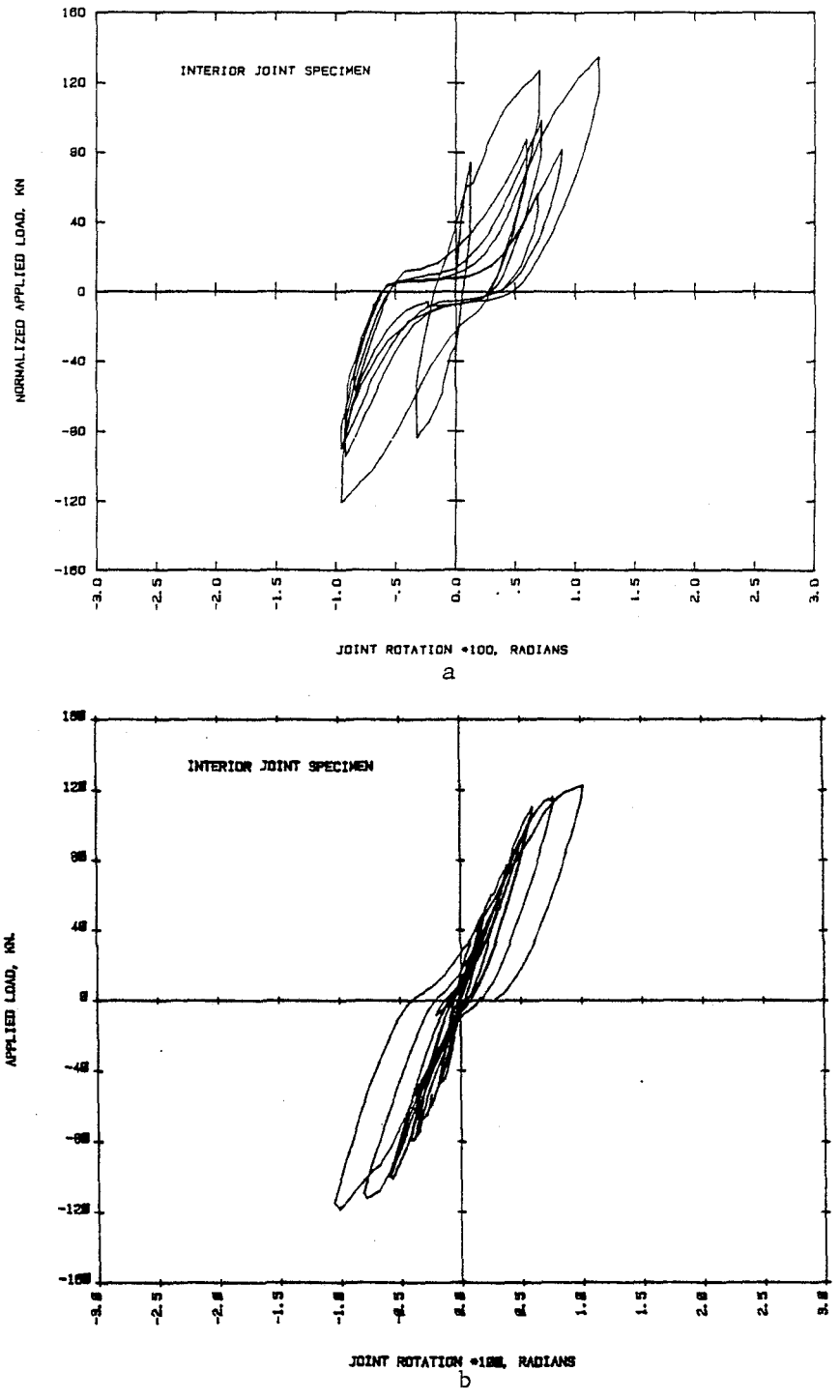

Fig. 4.10 Comparison of (a) Small-Scale and (b) Large-Scale Specimens

for the response of the small-scale specimens was normalized as previously described in Section 3.3.

Within the range of rotation of +-.010 radians, the small-scale specimens showed similar characteristics to the large-scale specimens with regard to a stiffness reduction at first cracking and a gradual stiffness degradation upon loading. Furthermore, unloading stiffnesses between the two scales matched very closely. The normalized maximum load of the small-scale specimens was 120 kN (27 kips), essentially the same as for large-scale specimens.

The good correlation between scales was not as evident in the load reversal range of the response (+-10kN). After just one load cycle into the nonlinear range, the small-scale specimens lost bond across the width of the column. The gradual stiffness degradation caused by progressive bond loss, which was characteristic of the large-scale specimens, was not modeled at small-scale. For the small-scale specimens, one complete large amplitude cycle was sufficient to pull the bar from each side of the joint in each direction, thereby destroying the bond. Bond resistance was hampered in the small-scale specimens for two reasons: first, mechanical anchorage was reduced because the wire which made up the reinforcement was smooth. Second, the tensile development length of the wire was approximately 130 mm (5 inches) based on pullout tests (45). This was considerably greater than the column width of 50 mm (2 inches). In the large-scale specimens the development length of the reinforcement was 460 mm (18 inches) based

on the ACI document 318-77 (16). This was equal to the width of the column. Future small-scale specimens may model prototype structures better if a wider column, small diameter wire, or some form of mechanical anchorage is used.

Subsequent load-cycles of the small-scale specimens revealed forms of behavior conistent with those described above. After the large-scale specimen had been put through enough large-amplitude cycles to completely destroy its bond, its response was very similar to that of the small-scale specimen. The small-scale specimens did exhibit some general trends which were characteristic of the large-scale specimens. Their strength and ability to deform were never exceeded, subsequent cycles to greater extremes caused reduced loading stiffnesses, unloading stiffnesses began high but decreased substantially near zero load.

In summary, the small-scale interior joint specimens did not model the hysteretic response of a large-scale specimen in the load reversal region of the response, until the large-scale specimen had gone through several large-amplitude loading cycles. Apart from this deviation, the small-scale specimens were able to mimic both the strength and the elastic stiffness characteristics of the large-scale specimens.

4.6 Comparison of Large and Medium-Scale Specimens

The load-rotation curves for the large and medium-scale specimens are shown in Fig. 4.11. The vertical axis of the response of the medium-scale specimen was normalized according to the

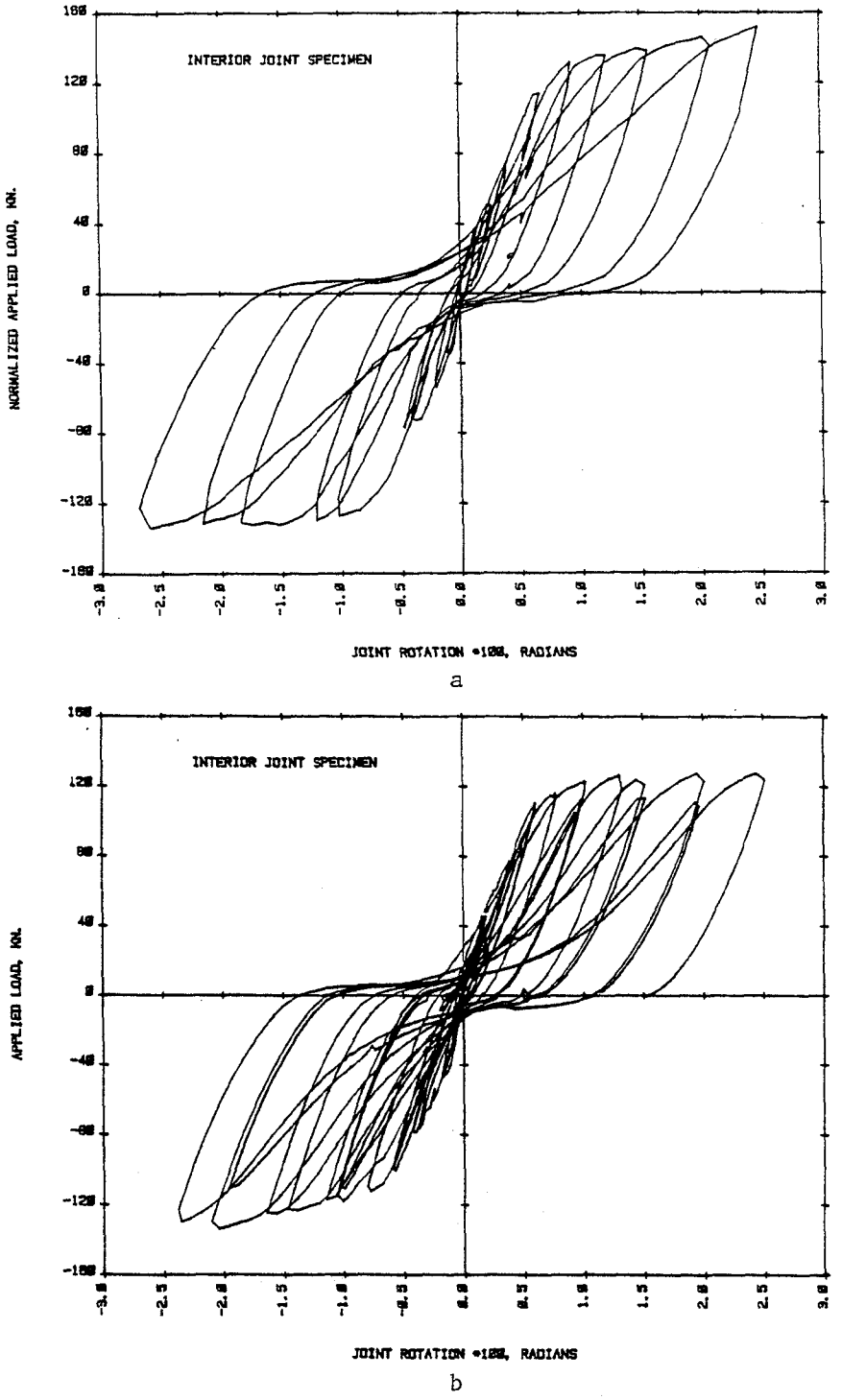

Fig. 4.11 Comparison of (a) Medium-Scale and (b) Large-Scale Specimens

procedure outlined in Section 3.3. In this case the length scale factor was 3.

The responses in Fig. 4.11 showed that all the stiffness characteristics exhibited by large-scale specimens were modeled well at 1/4-scale. Since conventional concrete was used in fabricating medium-scale specimens, cracking strengths between scales were essentially the same. Since standard deformed bars were used in the medium-scale specimens, the degradation in stiffness due to bar slip was modeled well. The only noticeable differences in the responses was in the normalized maximum load for the medium-scale specimens, which was slightly higher than the maximum load for the large-scale specimens. Unlike the small-scale, medium-scale models of beam-column joints showed they can be used to replicate behavior of full-scale prototypes well enough to be used as design aids.

CHAPTER 5

SUMMARY AND CONCLUSIONS

5.1 Summary

The purpose of this investigation was to determine if reduced scale models could depict the behavior of reinforced concrete beam-column joints under lateral load reversals. This was done by examining the differences in response of several test specimens. Specimens were constructed at large-scale (3/4-scale), medium-scale (1/4-scale), and small-scale (1/12-scale). Large-scale specimens were the control specimens. This investigator tested one large-scale exterior joint, two large-scale interior joints, and six medium-scale interior joints. One large-scale exterior joint and two large-scale interior joints were tested by others at the University of Colorado. All of these tests, combined with the results of tests of small-scale interior and exterior joints done at the University of Illinois, provided the data necessary to make comparisons. In this report data was presented for only one specimen of each scale and configuration because replication between like specimens was very good. Comparisons were based on the strength, stiffness, and energy dissipation characteristics exhibited by the hysteretic load-rotation relationship of each test specimen.

5.2. Conclusions

The results of the research have shown that a reduced-scale model of a beam-column joint can depict the response of a prototype within both the linear and nonlinear ranges. Specific conclusions and recommendations derived from the study are given below:

1) Reduced-scale specimens can be proportioned directly with the length scale factor. All depth, width, and cover dimensions can be scaled exactly. Allowance should be given to the percentage and strength of reinforcement.

2) Story shears resisted by a reduced-scale beam-column joint can be related to forces resisted by a large-scale specimen according to the following relations:

$$P_{LS} = \lambda^2 \frac{(\rho f y_{LS})}{(\rho f y_{RS})} V_{RS}$$

3) Scale relationships for small-scale specimens were highly dependent on the configuration of the component. For tests of exterior joints, where the longitudinal reinforcement was securely anchored in the joint region, overall stiffnesses and strengths were represented well by small-scale specimens. Tests of the interior joints did not show such good correlations between scales. Demand for more bond resistance was inherent for the interior joints because of the simultaneous push and pull on the beam reinforcement across the width of the joint. Bond degredation occurred at both small and large-scales, but to varying extents. Small-scale

specimens suffered complete bond loss after only one large amplitude loading cycle. The loss of bond in the large-scale specimens was more gradual. This demonstrated the need to develop a more effective means of anchorage for small-scale reinforcement. The ratio of the development length of reinforcement to the width of the column should be considered when designing specimens at small-scale. Use of small-scale specimens may be used to represent the hysteretic characteristics of a reinforced concrete beam-column joint for verification studies of numerical models. However, precise quantitative representations of these characteristics using a small-scale model may be inappropriate.

4) Bond degradation was found to be highly dependent on the development length of longitudinal reinforcing bars. In tests of large-scale specimens, one reinforced with #4 bars had significantly less bond loss with no loss in strength than those reinforced with #6 bars.

5) Specimens fabricated at 1/4-scale, using conventional concrete and standard deformed reinforcing bars, had very similar strength and stiffness characteristics to 3/4-scale specimens. Variance between load-rotation curves for large and medium-scale specimens was smaller than that for large-scale specimens reinforced differently. Furthermore, the variance was smaller for physical models constructed at 1/4-scale than that for numerical models and prototypes. Results of the research show that medium-scale specimens may be used directly for design and analysis of full-scale reinforced concrete frame structures.

5.3 Recommended Future Research

This study determined that simple components of two-dimensional reinforced concrete frame structures can be represented well by medium-scale models. Future research should focus on more complex structures to determine if similar scale relationships to those put forth in this report can be applied to a variety of components. Components which could be investigated should include unsymmetrically reinforced rectangular beams, T-beams, three-dimensional frames, walls, shell structures, and cable-stayed or segmentally prestressed bridges. Data from such tests could be used to verify existing nonlinear analysis techniques.

Future research should also concrete on the development of small-scale technology. It would be very advantageous to produce a 1/12-scale model which could predict the response of large-scale specimens as accurately as a 1/4-scale model.

The results of this study have shown it would be conceivable to test a 1/4-scale model of a concrete frame structure to examine the lateral load resistance in many full-scale structures. In a moderate-sized structural engineering laboratory, it would be feasible to test a model as tall as twenty stories.

BIBLIOGRAPHY

1. "Recommendations for a U.S.-Japan Cooperative Research Program Utilizing Large-Scale Testing Facilities", U.S.-Japan Planning Group Cooperative Research Program Utilizing Large-Scale Testing Facilities, Earthquake Engineering Research Center, University of California, Berkeley, Report No. 79-26, September, 1979.

2. Gulkan, P., and M.A. Sozen, "Inelastic Response of Reinforced Concrete Structures to Earthquake Motions", Journal of the American Concrete Institute, Vol. 71, No. 12, December, 1974, pp. 601-609.

3. Otani, S., and M.A. Sozen, "Simulated Earthquake Tests of R/C Frames", Journal of the Structural Division, ASCE, Vol. 100, No. ST3, March, 1974, pp. 687-701.

4. Aristizabal-Ochoa, J.D., and M.A. Sozen, "Behavior of Ten-Story Reinforced Concrete Walls Subjected to Earthquake Motions", Civil Engineering Studies, Structural Research Series No. 431, University of Illinois, Urbana, October, 1976.

5. Lybas, J.M., "Concrete Coupled Walls: Earthquake Tests", Journal of the Structural Division, Vol. 107, No. ST5, May, 1981, pp. 835-856.

6. Healey, T.J., and M.A. Sozen, "Experimental Study of the Dynamic Response of a Ten-Story Reinforced Concrete Frame with a Tall First Story", Civil Engineering Studies, Structural Research Series No. 450, University of Illinois, Urbana, August, 1978.

7. Moehle, J.P., and M.A. Sozen, "Earthquake-Simulation Tests of a Ten-Story Reinforced Concrete Frame with a Discontinued First-Level Beam", Civil Engineering Studies, Structural Research Series No. 451, University of Illinois, Urbana, August, 1978.

8. Abrams, D.P., "Experimental Study of Frame-Wall Interaction in Reinforced Concrete Structures Subjected to Strong Earthquake Motions", Seventh World Conference on Earthquake Engineering, Istanbul, Turkey, September, 1980.

9. Moehle, J.P., and M.A. Sozen, "Experiments to Study Earthquake Response of R/C Structures with Stiffness Interruptions", Civil Engineering Studies, Structural Research Series No. 482, University of Illinois, Urbana, August, 1980.

10. Stewart, J. and Abrams, D.P., "Comparison of Large and Small-Scale Reinforced Concrete Behavior", Masters Thesis, University of Colorado, July, 1982.

11. Bedell, R., and Abrams, D.P., "Scale Relationships of Concrete Columns", Structural Research Series No. 8302, Department of Civil Engineering, University of Colorado, Boulder, January, 1983.

12. Kreger, M.E., and D.P. Abrams, "Measured Hysteresis Relationships for Small-Scale Beam Column Joints", Civil Engineering Studies, Structural Research Series No. 453, University of Illinois, Urbana, August, 1978.

13. Gilbertsen, N.D., and J.P. Moehle, "Experimental Study of Small-Scale R/C Columns Subjected to Axial and Shear Force Reversals", Civil Engineering Studies, Structural Research Series No. 481, University of Illinois, Urbana, July, 1980.

14. Abrams, D.P., and M.A. Sozen, "Experimental Study of Frame-Wall Interaction in Reinforced Concrete Sructures Subjected to Strong Earthquake Motions", Civil Engineering Studies, Structural Research Studies No. 460, University of Illinois, Urbana, May, 1979.

15. Aktan, A.E., Bertero, V.V., Chowdhurry, A.A., and Nagashima, T., "Experimental and Analytical Predictions of the Mechanical Characteristics of a 1/5-Scale Model of a 7-Story Reinforced Concrete Frame-Wall Building Structure", Earthquake Engineering Research Center, University of California, Berkeley, Report No. 83-13, 1983.

16. "Building Code Requirements for Reinforced Concrete (ACI-77)", American Concrete Institute, Detroit, 1977.

17. Gavlin, N.L., "Bond Characteristics of Model Reinforcement", Civil Engineering Studies, Structural Research Series No. 427, University of Illinois, Urbana, April, 1976.

18. Newmark, N.M., "Current Trends in the Seismic Analysis and Design of High Rise Structures", Chapter 16 in Earthquake Engineering, Prentice-Hall, Inc. Englewood Cliffs, N.J., 1970, pp. 403-424.

19. Takeda, T., M.A. Sozen and N.N. Nielsen, "Reinforced Concrete Response to Simulated Earthquakes", Journal of the Structural Division, ASCE, Vol. 96, No. ST12, December, 1970, pp. 2257-2573.

20. Shibata, A., and M.A. Sozen, "The Substitute-Structure Method for Seismic Design in R/C", Journal of the Structural Division, ASCE, Vol. 102, No. ST1, January, 1976, pp. 1-18.

21. Biggs, J.M., W.K. Lau, and D. Persinki, "Aseismic Design Procedures for Reinforced Concrete Frames", Department of Civil Engineering, Massachusetts Institute of Technology, Publication No. R79-21, Order No. 653, July, 1979.

22. Derecho, A.T., S.K. Ghosh, M. Iqbal, and M. Fintel, "Strength, Stiffness, and Ductility Required in Reinforced Concrete Structural Walls for Earthquake Resistance", Journal of the American Concrete Institute, No. 8, Vol. 76, August, 1979, pp. 875-896.

23. Fintel, M., and S.K. Ghosh, "Aseismic Design of a 31-Story Frame-Wall Building", Proceedings of ASCE/Engineering Mechanics Division Specialty Conference: "Dynamic Response of Structures: Experimentation. Observation, Prediction, and Control", Atlanta, Georgia, January, 1981, pp. 874-886.

24. Saiidi, M. and M.A. Sozen, "Simple Nonlinear Seismic Analysis of R/C Structures", Journal of the Structural Division, ASCE, Vol. 107, No. ST5, May, 1981, pp. 937-952.

25. Tansirikongkol, V. and D.A. Pecknold, "Approximate Modal Analysis of Bilinear MDF Systems", Journal of the Engineering Mechanics Division, ASCE, Vol. 106, No. EM2, April, 1980.

26. Sozen, M.A., "Review of Earthquake Response of R/C Buildings with a View to Drift Control", Seventh World Conference on Earthquake Engineering, Istanbul, Turkey, September, 1980.

27. Wilby, G.K., "Response of Concrete Structures to Seismic Motions", Ph.D. Thesis, Department of Civil Engineering, University of Canterbury, Christchurch, New Zealand, July, 1975.

28. Hidalgo, P., and R.W. Clough, "Earthquake Simulator Study of a Reinforced Concrete Frame", Earthquake Engineering Research Center, University of California, Berkeley, Report No. 74-13, December, 1974.

29. Oliva, M.G., "Shaking Table Testing of a Reinforced Concrete Frame with Biaxial Response", Earthquake Engineering Research Center, University of California, Berkeley, Report No. 80-28, 1980.

30. Abrams, D.P., "Measured Hysteresis Relationships for Small-Scale Beams", Civil Engineering Studies, Structural Research Series No. 432, University of Illinois, Urbana, November, 1976.

31. Popov, E.P., V.V. Bertero and H. Krawinkler, "Cyclic Behavior of Three R.C. Flexural Members with High Shear", Earthquake Engineering Research Center, University of California, Berkeley, Report No. 72-5, October, 1972.

32. Soleimani, D., E.P. Popov and V.V. Bertero, "Hysteretic Behavior of Reinforced Concrete Beam-Column Subassemblages", Journal of the American Concrete Institute, No. 11, Vol. 76, November, 1979, pp. 1179-1196.

33. Viwathanatepa, S., E.P. Popov, and V.V. Bertero, "Seismic Behavior of Reinforced Concrete Interior Beam-Column Subassemblages", Earthquake Engineering Research Center, University of California, Berkeley, Report No. 79-14, June, 1979.

34. Vallenas, J.M., V.V. Bertero and E.P. Popov, "Hysteretic Behavior of Reinforced Concrete Structural Walls", Earthquake Engineering Research Center, University of California, Berkeley, Report No. 79-20, August, 1979.

35. Zagajeski, S.W., V.V. Bertero, and J.G. Bouwkamp, "Hysteretic Behavior of Reinforced Columns Subjected to High Axial and Cyclic Shear Forces", Earthquake Engineering Research Center, University of California, Berkeley, Report No. 78-05, 1978.

36. Hanson, N.W., and H.W. Conner, "Seismic Resistance of Reinforced Concrete Beam-Column Joints", Journal of the Structural Division, ASCE, Vol. 93, ST5, October, 1967, pp. 533-560.

37. Uzumeri, S.M., and M. Seckin, "Behavior of Reinforced Concrete Beam-Column Joints Subjected to Slow Land Reversals", Department of Civil Engineering, University of Toronto, Report No. 75-05, March, 1974.

38. Otani, S., and W.T. Cheung, "Behavior of Reinforced Concrete Columns Under Biaxial Lateral Load Reversals", Department of Civil Engineering, University of Toronto, Publication 81-02, February, 1981.

39. Jirsa, J.O., "Development of Loading System and Initial Tests: Short Columns under Bidirectional Loading", Department of Civil Engineering, University of Texas at Austin, CESRL Report 78-2, 1978.

40. Zia, P., R.N. White and D.A. VanHorn, "Principles of Model Analysis", Models for Concrete Structures, Special Publication of American Concrete Institute No. 24, 1970.

41. Staffier, S.R., and M.A. Sozen, "Effect of Strain Rate on Yield Stress of Model Reinforcement", Civil Engineering Studies, Structural Research Series No. 415, University of Illinois, Urbana, February, 1975.

42. Krawinkler, H., "Possibilities and Limitations of Scale-Model Testing in Earthquake Engineering", Proceedings of the Second U.S. National Conference on Earthquake Engineering, Earthquake Engineering Research Institute, August, 1979.

43. Moncarz, P.D., and H. Krawinkler, "Material Simulation in Dynamic Model Studies of Steel and Reinforced Concrete Structures", Seventh World Conference on Earthquake Engineering, Istanbul, Turkey, September, 1980.

44. Scholl, Roger E., ed., "EERI Delegation to the People's Republic of China", Earthquake Engineering Research Institute, Berkely, CA, January, 1982.

45. Kreger, M.F. and Sozen, M.A., "A Study of the Causes of Column Failures in the Imperial County Services Building During the 15 October 1979 Imperial Valley Earthquake". Civil Engineering Studies, Structural Research Series No. 509. University of Illinois, Urbana, August, 1983.

46. Wolfgram, Kathy, Report on 1/10-scale Model of Japanese Full-Scale 7-Story Test Structures, University of Illinois, 1984.

APPENDIX

Load-Rotation Curves

for Other Large-Scale Specimens

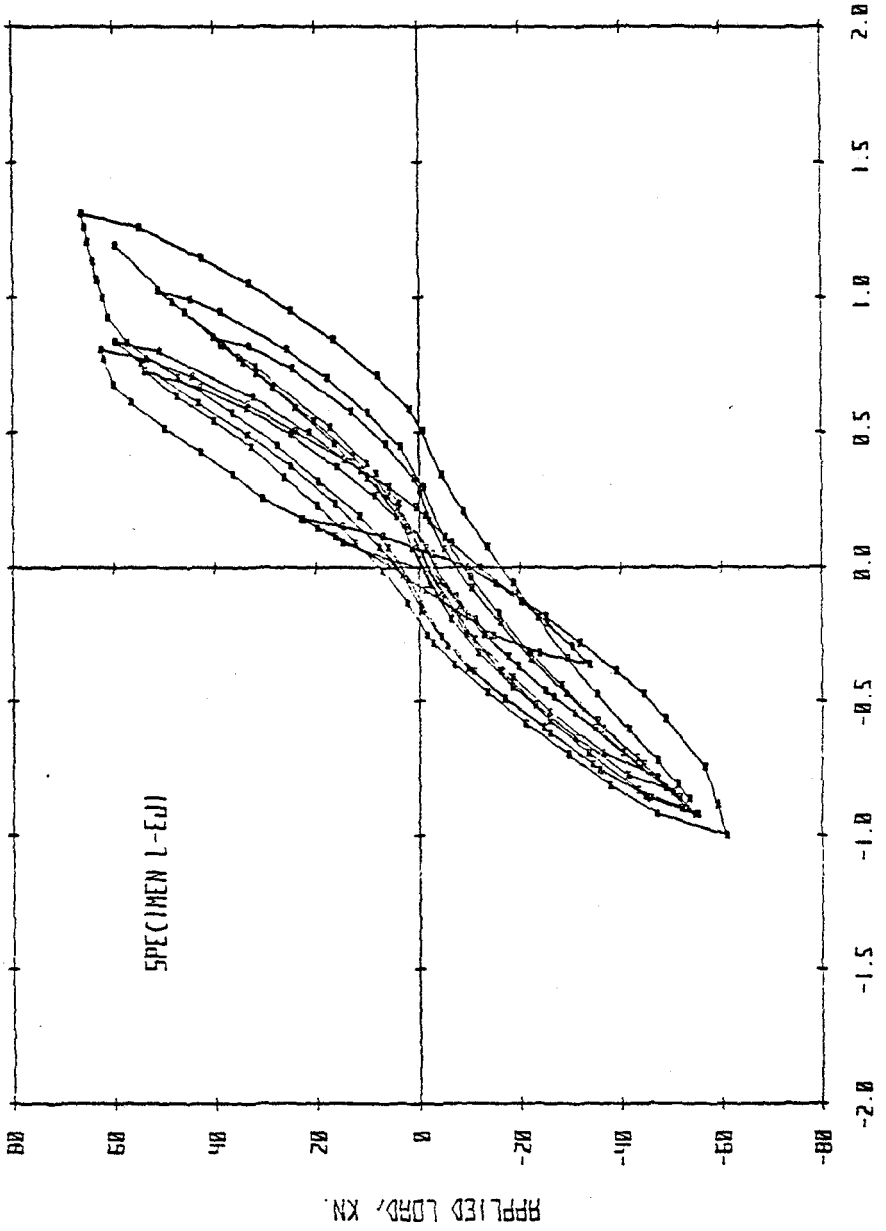

Fig. A.1 Load-Rotation Response for Specimen LEJ1

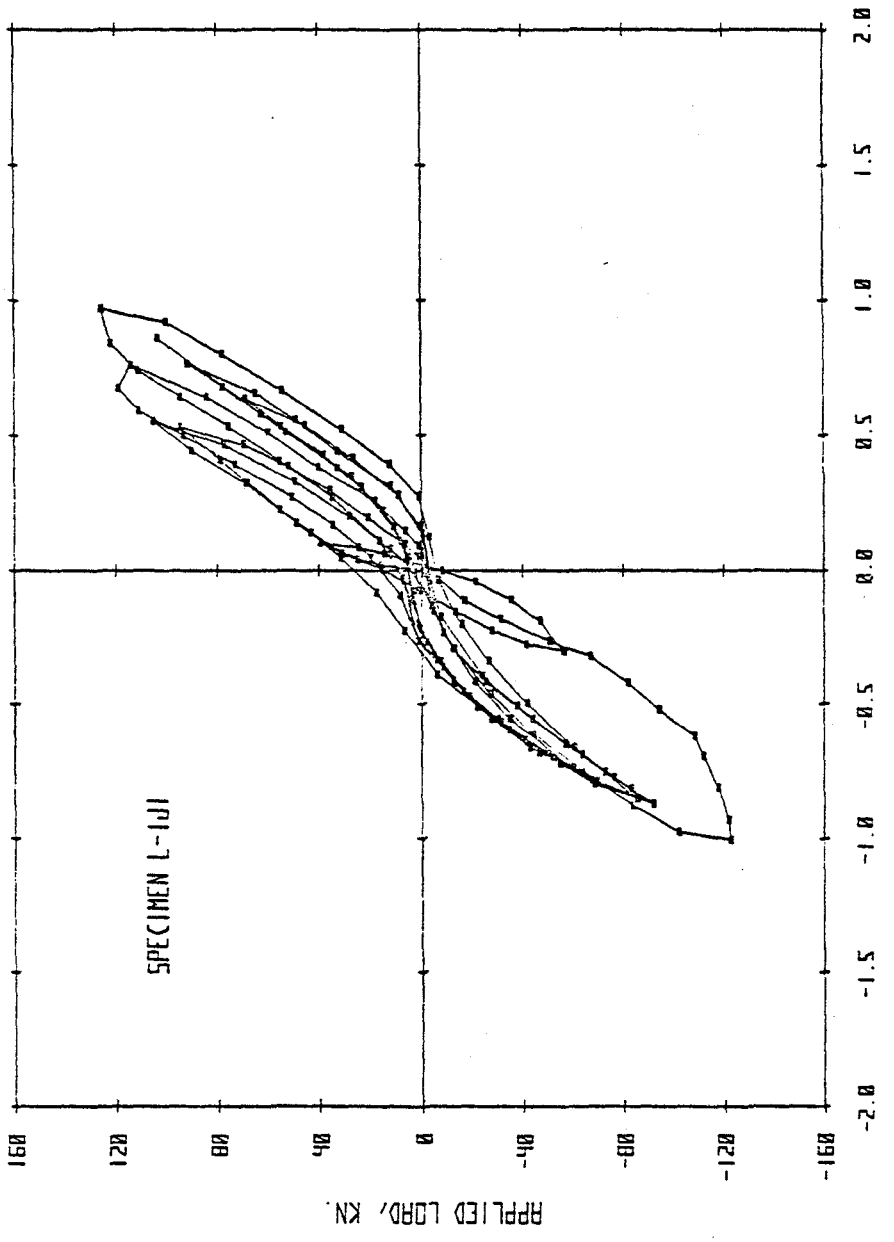

Fig. A.2 Load-Rotation Response for Specimen LIJ1

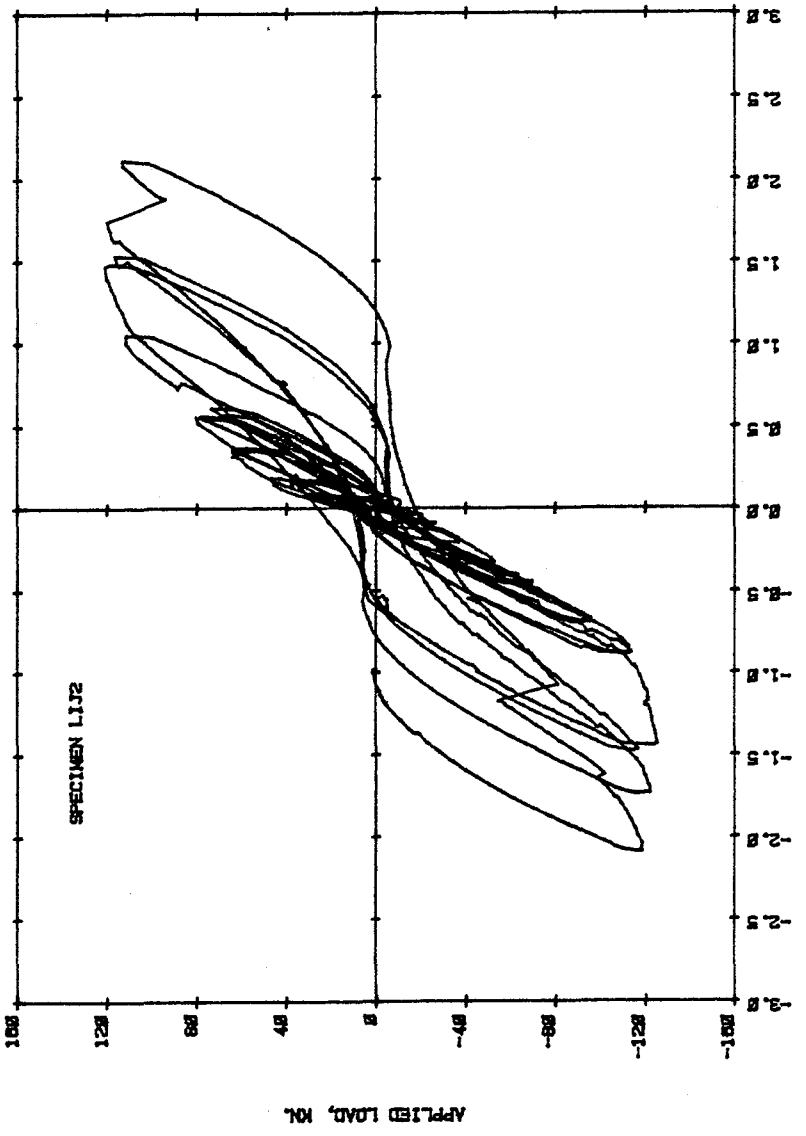

Fig. A.3 Load-Rotation Response for Specimen LIJ2